

New and comprehensive β - and βp -decay spectroscopy results in the vicinity of ^{100}Sn

J. Park,^{1,2,*} R. Krücken,^{1,2} D. Lubos,^{3,4,5} R. Gernhäuser,³ M. Lewitowicz,⁶ S. Nishimura,⁴ D. S. Ahn,⁴ H. Baba,⁴ B. Blank,⁷ A. Blazhev,⁸ P. Boutachkov,⁹ F. Browne,^{4,10} I. Čeliković,^{6,11} G. de France,⁶ P. Doornenbal,⁴ T. Faestermann,^{3,5} Y. Fang,¹² N. Fukuda,⁴ J. Giovinazzo,⁷ N. Goel,⁹ M. Górska,⁹ H. Grawe,⁹ S. Ilieva,¹³ N. Inabe,⁴ T. Isobe,⁴ A. Jungclaus,¹⁴ D. Kameda,⁴ G. D. Kim,¹⁵ Y.-K. Kim,^{15,16} I. Kojouharov,⁹ T. Kubo,⁴ N. Kurz,⁹ Y. K. Kwon,¹⁵ G. Lorusso,⁴ K. Moschner,⁸ D. Murai,⁴ I. Nishizuka,¹⁷ Z. Patel,^{4,18} M. M. Rajabali,¹ S. Rice,^{4,18} H. Sakurai,¹⁹ H. Schaffner,⁹ Y. Shimizu,⁴ L. Sinclair,^{4,20} P.-A. Söderström,⁴ K. Steiger,³ T. Sumikama,¹⁷ H. Suzuki,⁴ H. Takeda,⁴ Z. Wang,¹ H. Watanabe,²¹ J. Wu,^{4,22} and Z. Y. Xu¹⁹

¹TRIUMF, 4004 Wesbrook Mall, Vancouver, British Columbia, Canada V6T 2A3

²Department of Physics and Astronomy, University of British Columbia, Vancouver, British Columbia, Canada V6T 1Z1

³Physik Department, Technische Universität München, D-85748 Garching, Germany

⁴RIKEN Nishina Center, Wako-shi, Saitama 351-0198, Japan

⁵Excellence Cluster Universe, Technische Universität München, D-85748 Garching, Germany

⁶Grand Accélérateur National d'Ions Lourds (GANIL), CEA/DSM-CNRS/IN2P3, Boulevard H. Becquerel, 14076 Caen, France

⁷Centre d'Etudes Nucléaires de Bordeaux-Gradignan, 19 Chemin du Solarium, CS 10120, F-33175 Gradignan Cedex, France

⁸Institute of Nuclear Physics, University of Cologne, D-50937 Cologne, Germany

⁹GSI Helmholtzzentrum für Schwerionenforschung GmbH, D-64291 Darmstadt, Germany

¹⁰School of Computing, Engineering and Mathematics, University of Brighton, Brighton BN2 4GJ, United Kingdom

¹¹Vinča Institute of Nuclear Sciences, University of Belgrade, 11000 Belgrade, Serbia

¹²Osaka University, Machikaneyama-machi 1-1, Osaka 560-0043 Toyonaka, Japan

¹³Technische Universität Darmstadt, D-64289 Darmstadt, Germany

¹⁴Instituto de Estructura de la Materia, IEM-CSIC, E-28006 Madrid, Spain

¹⁵Rare Isotope Science Project, Institute for Basic Science, Daejeon 305-811, Republic of Korea

¹⁶Department of Nuclear Engineering, Hanyang University, Seoul 133-791, Republic of Korea

¹⁷Department of Physics, Faculty of Science, Tohoku University, Sendai 980-0845, Japan

¹⁸Department of Physics, University of Surrey, Guildford GU2 7XH, United Kingdom

¹⁹University of Tokyo, 7-3-1 Hongo Bunkyo, Tokyo 113-0033, Japan

²⁰University of York, York YO10 5DD, United Kingdom

²¹Beihang University, Beijing 100191, China

²²Department of Physics, Peking University, Beijing 100871, China



(Received 15 December 2018; published 14 March 2019)

A decay spectroscopy experiment on proton-rich nuclei in the vicinity of the doubly magic ^{100}Sn was carried out at RIKEN Nishina Center. More than 20 nuclei with $43 \leq Z \leq 50$ and $N \leq 51$, produced by fragmentation reactions were investigated via analyses of β -decay, βp -decay, and subsequent γ -ray data. Owing to higher statistics, the precision on the half-lives of many of the ground states and isomers was improved. β -decay endpoint energies of 11 states in 8 nuclei were measured for the first time, and the corresponding Q_{EC} and excitation energies were generally consistent with various mass models. Many β -delayed proton emission branching ratios were measured either for the first time or with higher precision compared to literature values, and some of them differed by more than 2σ . Many of the large discrepancies were associated with nuclei with long-lived isomeric states, highlighting large systematic uncertainties involved in these measurements. Twenty-five new γ rays were observed, and ten new states are proposed with unambiguous excitation energies, spins, and parities. Most of the energies of the excited states were consistent within 300 keV or 20%, whichever was greater, compared to shell model predictions in the proton/neutron ($p_{1/2}$, $g_{9/2}$) model space assuming a ^{76}Sr core. A signature of a new $(1/2^-)$ isomer in ^{97}Cd with $T_{1/2} = 0.73(7)$ s was found, in good agreement with shell model predictions.

DOI: [10.1103/PhysRevC.99.034313](https://doi.org/10.1103/PhysRevC.99.034313)

I. INTRODUCTION

Multiple research topics in nuclear structure and nuclear astrophysics converge on the heaviest bound $N = Z$ magic nucleus ^{100}Sn and its neighboring proton-rich nuclei [1]. These nuclei are bound against proton emission by only a

*Present address: Department of Physics, Lund University, 22100 Lund, Sweden; joochun.park@nuclear.lu.se

few MeV, and experimentally observable quantities such as excitation energies (E_x), Gamow-Teller (GT) decay strengths B_{GT} , and electromagnetic (EM) transition strengths are used to assess quantitatively the robustness of the ^{100}Sn core. Previous experiments on these nuclei have yielded insightful and/or controversial results [2–5], highlighted by the GT decay of ^{100}Sn with the smallest $\log ft$ value of all known β decays [6]. In the context of nuclear astrophysics, experimental half-lives ($T_{1/2}$) and β -delayed proton branching ratios ($b_{\beta p}$) are needed for reaction flow calculations of the rapid-proton (rp) capture process of nucleosynthesis via type I x-ray bursts and steady-state burning [7–9]. The dependence of elemental abundances of $A \sim 100$ nuclides on these quantities has been discussed in Refs. [4,10].

Various types of shell model (SM) calculations have been performed to describe the nuclear properties of isotopes near the $N = Z = 50$ double shell closure: empirical shell models (ESMs) [11–15] in the proton (π) and neutron (ν) model space of $p_{1/2}$ and $g_{9/2}$ orbitals above the ^{76}Sr core; and large-scale shell model (LSSM) calculations involving higher-lying orbitals above the ^{100}Sn core [5,6,16–18]. They have been adopted and tuned to reproduce the energies and EM transition strengths of core-excited states in this region [18–22]. One research topic of interest is the competition between collective phenomena driven by the $T = 0$ proton-neutron (pn) interaction and the seniority scheme built on pp and nn pairs as a function of the $g_{9/2}$ orbital occupation number.

The current experimental knowledge of the mass, structure, and decay properties of the nuclei in this region is not exhaustive. Predictions of $1/2^-$ isomers in odd-mass nuclei formed by a hole in the $p_{1/2}$ orbital have been confirmed in only a few nuclei, and even macroscopic quantities such as half-lives and masses are either unknown or limited in precision. However, the improved production rate of these exotic nuclei at various accelerator facilities has enabled a more detailed investigation and a possibility to determine the proton dripline of the heaviest $N \sim Z$ nuclei [23]. This article presents a comprehensive set of experimental β -decay endpoint energies (Q_β), $T_{1/2}$, $b_{\beta p}$, and deexcitation γ rays of proton-rich nuclei for $43 \leq N, Z \leq 51$. They are compared with the literature values and discussed in the framework of ESM where applicable.

II. EXPERIMENT AND ANALYSIS

A. Isotope production and identification

The proton-rich nuclei in the ^{100}Sn region were produced by fragmentation reactions of a 345-MeV/ u ^{124}Xe primary beam on a ^9Be target at the Rikagaku Kenkyusho (RIKEN, The Institute of Physical and Chemical Research) of Japan RI Beam Factory [24]. The thickness of the target was 740 mg/cm², and the average primary beam intensity was 30 pA. At the first stage of BigRIPS, a 3-mm Al wedge degrader, dipole magnets, and slits at the dispersive foci separated out unwanted fragments by the $B\rho$ - ΔE - $B\rho$ method. At the later stages of BigRIPS and the ZeroDegree spectrometer, $B\rho$ -ToF- ΔE measurements with position-sensitive parallel-plate avalanche counters [25], plastic scintillators,

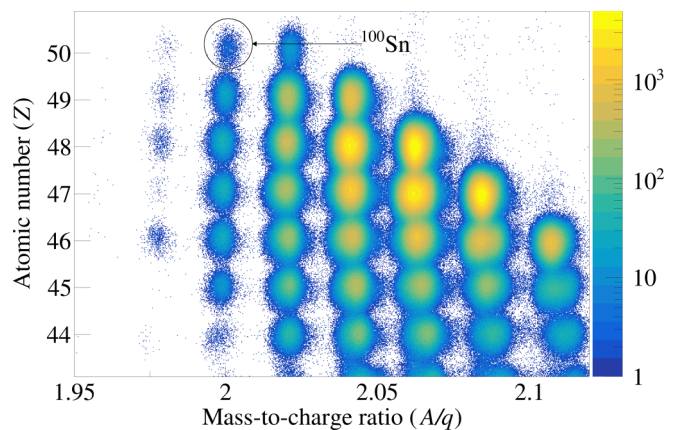


FIG. 1. Particle identification plot of proton-rich radioactive nuclei produced in this experiment. ^{100}Sn is marked as a reference.

and a gas-filled ionization chamber [26] were carried out to identify the remaining radioactive isotopes with different mass-over-charge ratios A/q and atomic number Z on an event-by-event basis [27,28]. A particle identification plot of radioactive isotopes produced in this experiment during ~ 200 h of beam time is shown in Fig. 1. At this primary beam energy, more than 90% of the identified ions are fully stripped ($Z = q$) for low levels of background contamination in particle identification [29].

B. Heavy ion implantation and decay correlation

The radioactive beam was implanted in one of the double-sided silicon strip detectors (DSSSDs) of the wide-range active silicon strip stopper array for beta and ion detection (WAS3ABi) [30]. WAS3ABi consisted of a stack of three DSSSDs and ten single-sided silicon strip detectors (SSSSDs) serving as β calorimeters placed further downstream of the DSSSDs with equal dimensions and thicknesses. Each DSSSD was 1 mm thick and segmented into 60 and 40 strips with 1-mm widths in x and y directions, respectively. The fine segmentation enabled a position-sensitive implantation-decay correlation scheme. The position of each implanted radioactive ion (RI) was determined by identifying the x -side strip with the minimum time-to-digital converter (TDC) value where $\Delta T = T_{\text{strip}} - T_{\text{trigger}}$, and the y -side strip with the maximum ΔE . The DSSSD number in which the RI was implanted was determined by noting the most downstream DSSSD with at least 10 MeV deposited in a single strip. The majority of the RI beam was implanted in the middle DSSSD as intended and governed by kinematics. γ rays following decay events were detected with the Euroball-RIKEN Cluster Array (EURICA) [31], which consisted of 84 high-purity germanium crystals arranged in 12 clusters that surrounded WAS3ABi in a 4π geometry. The time window for γ -ray detection which was opened by a global trigger from a DSSSD signal was 12 μs . Standard ^{60}Co and ^{152}Eu radioactive sources were used to calibrate WAS3ABi and EURICA in energy. After having calibrated the EURICA detectors, WAS3ABi-EURICA coincidence events of Compton-scattered γ rays inside the silicon strips of WAS3ABi were

analyzed for an accurate energy calibration in the range of 100–1200 keV.

β and βp decay events were correlated to ion implantation events if the decay event deposited at least 100 keV within a one-pixel distance from the implantation position in the same DSSSD. This energy threshold was applied in the offline analysis in order to suppress thermal noise events constituting random background correlations. In addition to the spatial correlation window, the time correlation window was set between -20 and 20 s after ion implantation. The negative time window allowed the characterization of the random background correlations [32], and the 20-s cutoffs were generally long enough compared to the half-lives of isotopes studied in this work.

C. Decay $T_{1/2}$ analysis

Decay time distributions of both β and βp decays of isotopes with $T_{1/2} < 20$ s were analyzed. The half-life analysis of the isotopes was required not only for the $T_{1/2}$ needed for $\log ft$ and B_{GT} measurements, but also for isomeric ratios and $b_{\beta p}$ where applicable. Furthermore, γ -ray intensities normalized to the total number of decays can be used to cross-check the consistency in detector efficiencies and quantify missing/direct ground-state decay branching ratios. In order to simplify the analysis, the decay events were first classified as either β decays or βp decays as described in Sec. III E.

The $T_{1/2}$ analysis of the proton-rich nuclei presented in this article involved two distinct strategies: multiparameter fits on the total decay time distribution with a Bateman equation [33], and a simple exponential decay fit on γ -ray gated decay time distributions. The first approach was applicable to the isotopes with low production statistics and/or low-intensity β - and βp -delayed γ -ray branches. With a few exceptions, the absence of βp emitters in the descendant generations simplified the fit functions for βp decay analyses. The $T_{1/2}$ and b_{EC} of the β - and βp -daughter nuclei in the Bateman equation were allowed to vary within 2σ uncertainties based on the literature values listed in the NUBASE2016 database [34] and Evaluated Nuclear Structure Data Files (ENSDF) for $A = 87$ – 100 isotopes [35–48]. The fit parameters of the parent decay function were free. Within the finite time window, contributions from the granddaughter decay components were negligible.

A significant fraction of the isotopes produced in this experiment were populated in isomeric states which have half-lives comparable to those of the ground states, and for certain nuclei their $T_{1/2}$ and b_{EC} have not been measured precisely in the past. These uncertainties would propagate and lower the attainable precision of the parent decay half-lives. To resolve the aforementioned challenges in the $T_{1/2}$ analysis, selection cuts were applied on previously identified γ -ray transitions assigned to the daughter nucleus. Then high-purity distributions of β - and βp -decay times of the parent state(s) were fitted. Often the reduction of the number of fit parameters compensates for the lost statistics, which is dependent on the EURICA efficiencies at the corresponding γ -ray energies and internal conversion (IC) coefficients of the EM transitions.

D. Q_β measurements

The mass excess differences between the parent and the daughter nuclei were determined by measuring Q_β in the following relationship:

$$\Delta m({}_Z^A X) - \Delta m({}_{Z-1}^A X) = Q_{EC} = Q_\beta^x + E_x + 2m_e, \quad (1)$$

where Δm is the mass excess, Q_{EC} is the ground-state-to-ground-state energy difference, and Q_β^x is the β -decay endpoint energy for a particular final state x in the daughter nucleus with energy E_x .

The determination of Q_β of the exotic nuclei with WAS3ABi was limited to a few cases due to three major reasons: an incomplete calorimetry of positrons with WAS3ABi, an imprecise knowledge of the β -decay branching ratios b_β , and contaminants of the E_β spectrum due to β decays from isomers/daughter nuclei and random correlations. The first disadvantage has been addressed by generating simulated E_β distributions at different trial Q_β in Geant4 with a simulated geometry of WAS3ABi [49,50] and finding the closest match with the experimental spectra via χ^2 minimization. The χ^2 trends as a function of trial Q_β were fitted with third-degree polynomials, and the uncertainties on Q_β were determined by finding the two trial Q_β values where $\chi^2 = \chi_{\min}^2 + 1$. Heavy-ion implantation position distributions for each nucleus of interest were properly implemented in the simulations. The other two obstacles could be adequately handled in two cases: the superallowed Fermi β decays from the ground states of odd-odd $N = Z$ species ${}^{90}\text{Rh}$, ${}^{94}\text{Ag}$, and ${}^{98}\text{In}$; and the existence of a dominant β -decay branch to an excited state which was not fed from above and could be tagged with specific γ -ray gates. The results are presented in Sec. III C.

In the case of superallowed Fermi decays, it was assumed that 100% of the β decays from the 0^+ state in the parent nucleus would populate the 0^+ isobaric analog state in the daughter nucleus. Contamination from background decays was characterized by sampling the E_β spectrum with different time gates and scaling each subset based on the cumulative distribution function derived during the $T_{1/2}$ analysis for each decay component (random background, β daughter, βp daughter, etc.). Then the contamination spectrum was subtracted from the total E_β distribution before the χ^2 comparison with simulated data. This procedure could be carried out with little loss in statistics due to the small $T_{1/2}$ (≈ 30 ms) of the Fermi-decaying ground states compared to the isomer, daughter, and random background decays with $T_{1/2} \geq 1$ s.

Alternatively, contaminants in the E_β spectrum could be suppressed by gating on β -delayed γ -ray transitions. Specific β -decay branches in Eq. (1) could be selected, eliminating large systematic uncertainties arising from poorly known b_β^x and Q_β^x . To minimize the effect of the Pandemonium problem [51] of unobserved β decays populating higher-energy states, gates were placed on γ -ray transitions from the highest excited state known so far. Contributions from background decays were characterized and subtracted from the total spectrum by setting γ -ray gates on the sides of the main peaks and sampling the γ -gated spectrum for $T_\beta < 0$. While the loss in statistics due to EURICA efficiency and low β -decay branching ratios (b_β) was too severe for many isotopes and

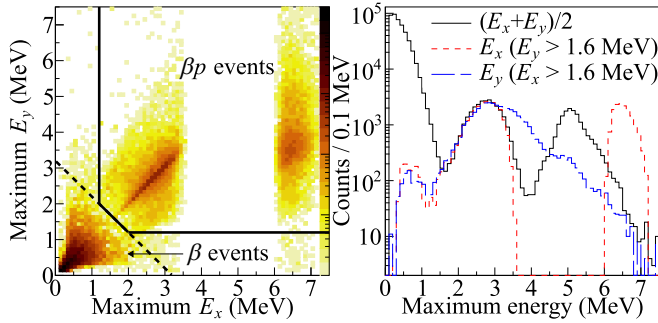


FIG. 2. Left: maximum energies deposited in x - and y -side DSSSD strips for decays correlated to ^{97}Cd implantation events. The void where $3.5 < E$ (MeV) < 6.0 on the x -side strips is due to an ADC saturation of the x -side strip channels, resulting in overflow events appearing at $E > 6$ MeV. Right: energy projections of the 2D matrix on the left. See Sec. II E for details.

isomeric states, several of them were available for reasonable Q_β analyses.

E. Identification of βp events and $b_{\beta p}$ analysis

Taking advantage of the high $\langle dE/dx \rangle$ of protons compared to positrons, decay events accompanying proton emission were identified by examining the energy deposition in thin silicon strips. The energy selection cut on βp events is illustrated in the left plot of Fig. 2, which shows the maximum energy deposits in x and y strips of the DSSSD for decay events correlated to ^{97}Cd implantations. In order to be classified as a proton emission event, a threshold of $(\Delta E_x + \Delta E_y)/2 > 1.6$ MeV (diagonal dashed line in Fig. 2) was applied. Furthermore, as seen in the histograms with dashed lines on the right side of Fig. 2, an energy deposition of at least 1.2 MeV was required in a DSSSD strip in both the x and y directions to be designated as βp events. The low-energy bumps are likely caused by multiscattering positrons inside a single strip oriented in either direction. Note that a significant fraction of βp events saturated the analog-to-digital converter (ADC) channels of the x -side strips of the DSSSDs, resulting in nonphysical overflow values and rendering the high-energy measurements on the x -side strips useless. Therefore the β -delayed proton energy spectra shown in Fig. 8 were generated from the maximum energies registered on the y -side strip only.

Then $b_{\beta p}$ values were determined from the number of βp decays divided by the total number of decays for each given state (ground state or isomer), determined from the $T_{1/2}$ analysis described in Sec. II C. Detector deadtime correction factors were applied, which ranged between 5% and 10% for all nuclei presented in this work. The number of β decays, required for determining isomeric ratios, was corrected for the β -decay correlation efficiency of the DSSSD in the range of 60–90%. Factors affecting the correlation efficiency were the heavy ion implantation profile distribution and the β -decay energy distribution. The βp decay correlation efficiency was assumed to be 100% due to the high $\langle dE/dx \rangle$ value of protons, which was supported by Geant4 simulations

scanning over various proton energies and ion implantation depths.

III. RESULTS AND DISCUSSION

The following subsections contain a summary of experimental $T_{1/2}$, Q_β , and $b_{\beta p}$ obtained from the experiment, followed by the β - and βp -delayed γ -ray spectroscopy results of nuclei of interest. The intensities of the γ rays (I_γ) reported in subsequent tables were normalized to the number of observed decays for either the β branch or the βp branch. Unless otherwise stated, isomeric ratios were applied to distinguish the contributions from both the ground state and the isomer of a given nucleus. Low-energy EM transitions were also corrected for IC in the intensity analysis, specified in their respective tables. Due to the large energy available for β decays of these nuclei and a finite γ -ray detection efficiency of EURICA, β -decay branching ratios deduced via I_γ are susceptible to the Pandemonium effect [51]. Consequently, the log ft values presented in this article are “apparent” values. Comparisons to literature and theories are discussed in individual subsections, and finally an overall evaluation of the agreement between SM and a large set of experimental E_x is presented in Sec. III Q. On the other hand, new β -delayed γ -ray spectroscopy results for ^{99}In and ^{101}Sn were also obtained from this experiment. However, they require discussions with SM calculations beyond the model space permitted by the SLGM interaction, and will be addressed in separate publications.

A. SM calculations

The experimental results are compared with SM calculations involving a ^{76}Sr core and $\pi\nu(p_{1/2}, g_{9/2})$ model space, adopting the single-particle energies (SPEs) and the two-body matrix elements (TBMEs) derived by Serduke, Lawson, and Gloeckner (SLG) [12]. Through the rest of the article, unless otherwise stated, “SM” refers to the calculation results based on the SLGM interaction which is the isospin-asymmetric interaction of SLG. SLGM is implemented in the computation software NUSHELLX [52]. The SPEs (in MeV) for the valence orbitals of the SLGM interaction are 0.766 ($\pi 2p_{1/2}$), -0.378 ($\pi 1g_{9/2}$), -8.699 ($\nu 2p_{1/2}$), and -9.271 ($\nu 1g_{9/2}$). The calculated energies of the low-lying states in one-nucleon hole nuclei ^{99}In , ^{99}Sn , and the doubly magic nucleus ^{100}Sn are shown in Fig. 3. Both the Q_{EC} of ^{99}Sn (14.30 MeV) and the S_p of ^{100}Sn (2.99 MeV) predicted by SLGM agree reasonably well with the AME2016 extrapolations of 13.43(59) and 3.20(42) MeV, respectively.

The same interaction had been used to predict EM transition strengths of γ -decaying isomers in this region of nuclides [22]. In this work, the magnetic moment g factors and the effective charges for predicting EM transition strengths were fixed at $g_{s,p} = 5.586$, $g_{s,n} = -3.826$, $g_{l,p} = 1$, $g_{l,n} = 0$ and $e_p = 1.5e$, $e_n = 0.5e$. Theoretical b_β and log ft values were calculated using the liquid drop model for the Q_{EC} value of the parent nucleus and the expression $ft = 6177/[(g_A/g_V)^2 B_{\text{GT}} + B_F]$, where B_F is the Fermi decay

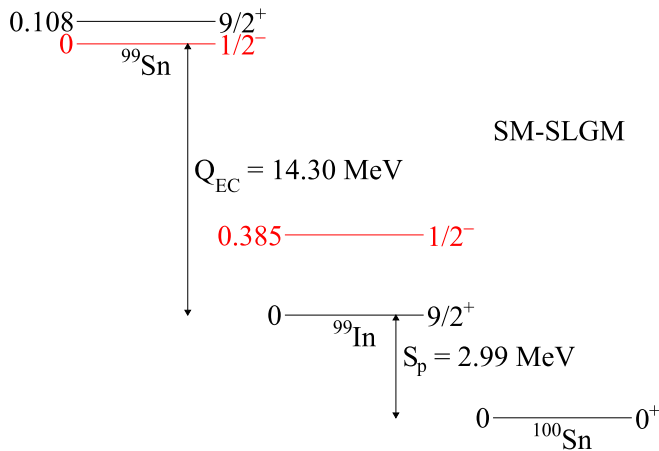


FIG. 3. Theoretical energies of the states in ^{99}In , ^{99}Sn , and ^{100}Sn from SM calculations with the SLGM interaction. The excitation energies are in MeV, and the energy gaps between different nuclei are not drawn in scale.

strength and $g_A/g_V = 1.260$ as implemented by default in NUSHELLX.

B. $T_{1/2}$ measurements

The β - and βp -decay $T_{1/2}$ measured in this work are presented in Figs. 4 and 5 and Table I. Due to the similar half-lives and lack of statistics for ^{88}Tc , ^{91}Ru , and ^{91}Rh , only combined $T_{1/2}$ including contributions from both the ground state and the isomeric state could be measured. In the case where independent $T_{1/2}$ could be measured from β -decay and βp -decay analyses, the weighted average of the two values was obtained.

All of the half-lives measured in this work are consistent with the literature values within 2σ except for ^{92}Rh and its isomer (see Sec. III K for details). For most states, the higher production statistics led to a higher precision.

The ground states of ^{90}Rh , ^{94}Ag , and ^{98}In have been known to undergo fast ($T_{1/2} < 100$ ms) β decays, presumably corresponding to the superallowed $0^+ \rightarrow 0^+$ Fermi decays. The relative precision on their $T_{1/2}$ was improved by at least a factor of 3 compared to the literature values. Nevertheless, in order to involve these heaviest odd-odd $N = Z$ nuclei in the discussion of the constancy of the ft value and the unitarity of the CKM matrix [57], much more precise $T_{1/2}$, b_β , and especially Q_{EC} values are required.

C. Q_β results for Q_{EC} and E_x

Experimental Q_β values were obtained for 8 nuclei and 11 states, as shown in Fig. 6. The asymmetric coverage of WAS3ABi is reflected in the energy spectra, where the majority of counts below 1 MeV is due to positrons traveling upstream relative to the beam direction. The γ -ray gates used to generate the Q_β spectra and the E_x of the final states are listed in Table II. The Q_{EC} were deduced according to Eq. (1), and the excitation energies of the isomers were determined by taking the Q_β differences between the ground state and the

isomer, as well as accounting for the differences in the final state energies.

The experimental Q_{EC} were then compared with the following mass models: the finite-range droplet macroscopic model (FRDM12) [59]; the Duflo-Zuker model with 33 parameters (DZ-33) [60], the Hartree-Fock-Bogoliubov mass calculation with 27 parameters (HF27) [61], and the Koura-Tachibana-Ueno-Yamada mass formula (KTUY05) [62]. The root-mean-square deviations provided either in the above references or discussed in separate articles [63,64] were adopted as individual mass excess uncertainties. AME2016 provided its own uncertainties on the extrapolated Q_{EC} . In addition, shell model calculation results by the SLGM interaction and the work by Herndl and Brown (HB, Ref. [15]) based on the isospin-symmetric SLGT interaction were also compared with the experimental data. The excitation energies of the three isomers are compared with those proposed in NUBASE2016 [34], SLGM, and HB. Conservative theoretical uncertainties of 400 keV were assigned to the two sets of SM calculations. The measured Q_{EC} and E_x are generally consistent with the predictions, as shown in Fig. 7. The most significant discrepancy in Q_{EC} was found in ^{98}In , but it is still within 2σ of several models. Concerning the masses of the lightest $Z = 49$ isotopes, ^{97}In has already been suggested to be more bound compared to the lighter odd- Z , $N = Z - 1$ nuclei ^{89}Rh and ^{93}Ag [65]. More precise mass measurements of indium isotopes within the ^{100}Sn core ($N \leq 50$) will answer whether they are more bound than predicted.

The experimental ft values of the superallowed β decays from ^{90}Rh , ^{94}Ag , and ^{98}In were determined to be 4270_{-2160}^{+2950} , 4170_{-1060}^{+1250} , and $3720(690)$, respectively. With their large uncertainties, these values are slightly higher but consistent with raw ft values in the range of 3030 and 3090 [57].

D. $b_{\beta p}$ measurements

The time distributions of βp decays and their half-life fits are shown in Fig. 5. The $T_{1/2}$ results and the $b_{\beta p}$ of the βp emitters are summarized in Table I. New $b_{\beta p}$ were determined for the (7^+) isomer in ^{90}Rh , the (2^+) isomer in ^{92}Rh , and the ground states of $^{92,95}\text{Pd}$ and ^{98}In . The $b_{\beta p}$ values of the (8^+) ground state and the (2^+) isomer in ^{96}Ag were measured by adopting the literature $T_{1/2}$ of 6.9(5) s [34] for the isomeric state in the overall βp decay half-life analysis.

For the nuclei with βp decay events less than 2σ above the background counts, upper limits on $b_{\beta p}$ were assigned by the following expression: $b_{\beta p} < 2\sqrt{N_{\text{bgd}}^{\beta p} + 4/N_{\text{state}}}$, where $N_{\text{bgd}}^{\beta p}$ is the number of random background βp events within the time window up to five times the $T_{1/2}$ of the parent state and N_{state} is the number of decays of a given state in a nucleus—either the ground state or the isomer(s). The addition of four counts (a little more than twice the upper uncertainty on 0 events [66]) was used to deduce the minimum threshold on the upper limit at the 2σ level if the βp decay time distribution was completely free of random background events. For the odd-odd $N = Z$ nuclei ^{90}Rh , ^{94}Ag , and ^{98}In , the βp decay times are plotted on a logarithmic scale and the fits were

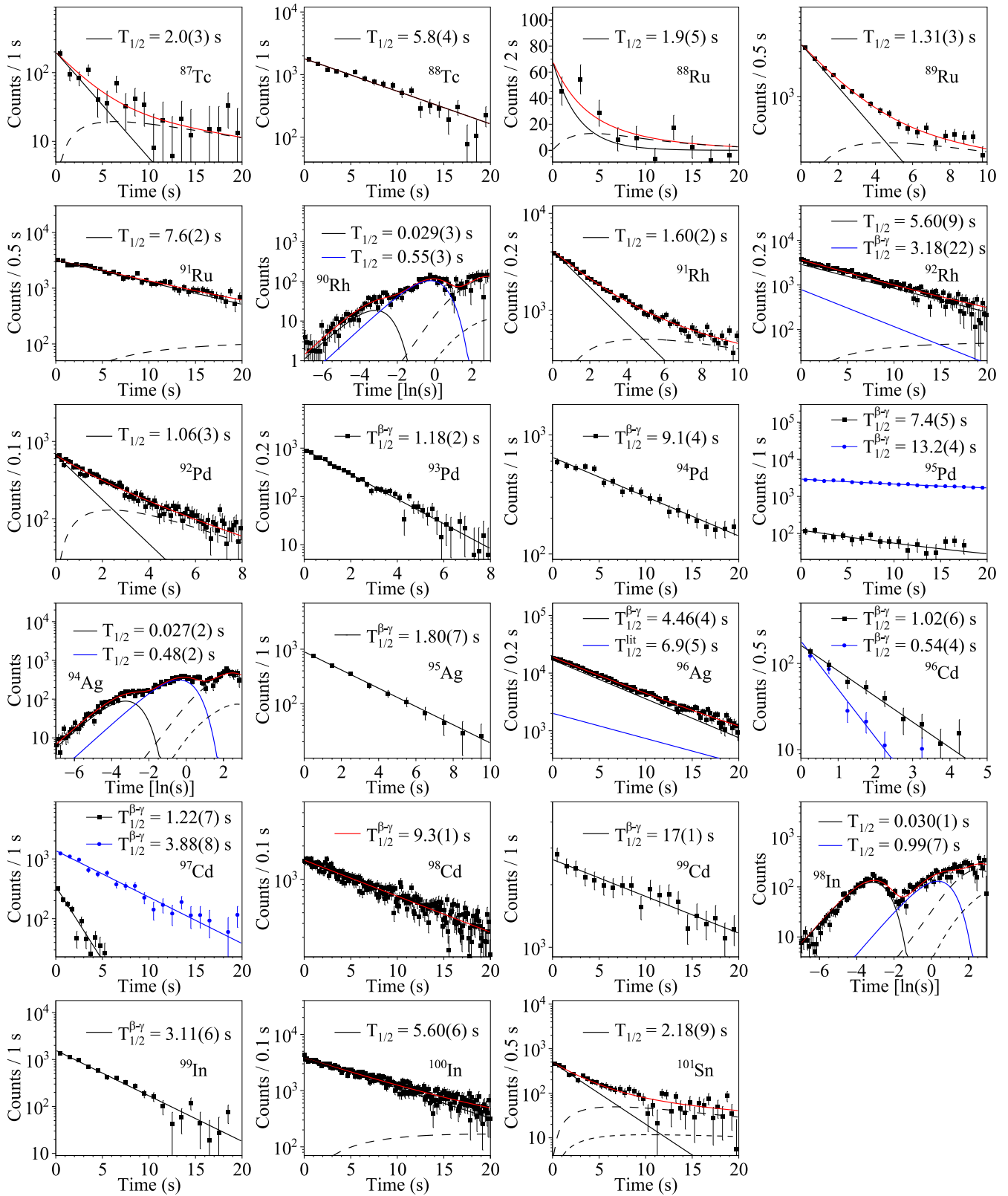
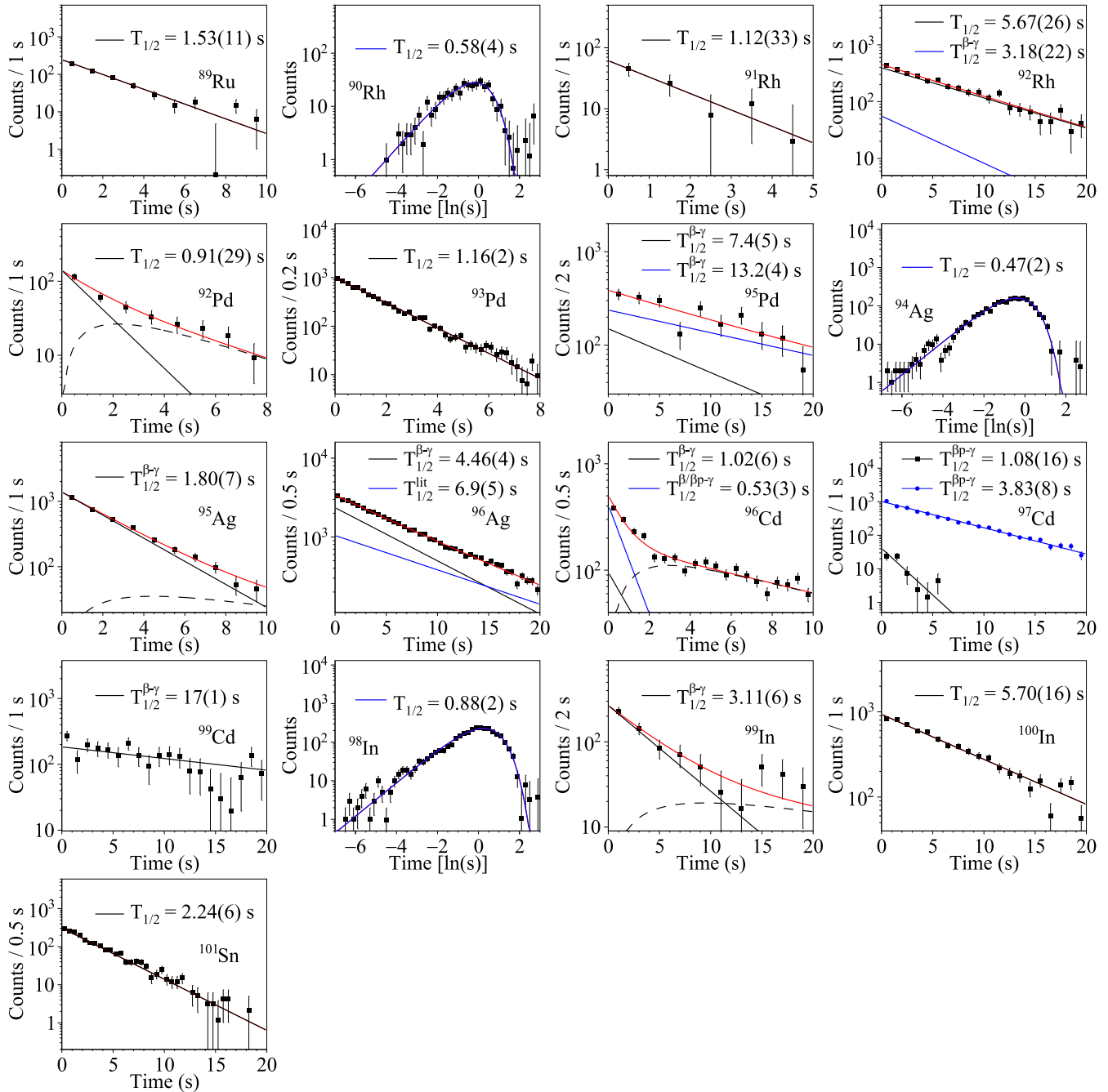


FIG. 4. β -decay time distributions of individual nuclei studied in this work. Red solid lines represent the fit functions containing all the decay components. The solid and the dashed lines correspond to the β -decay components of the ground state (black) and the isomers (blue) of the parent and the daughter nuclei, respectively. The long dashed lines represent the decays of the β -decay daughter nuclei, and the short dashed lines represent the decays of the βp -decay daughter nuclei. $T_{1/2}$ displayed with γ superscripts were determined from γ -gated β -decay time distributions. For the (2^+) isomer in ^{96}Ag , the literature half-life of 6.9(5) s [34] was adopted in order to determine the $b_{\beta p}$ value of the isomer.

FIG. 5. Same plot and description as Fig. 4, but for βp decay events.

performed using the Schmidt method [66] to investigate βp emission from their superallowed Fermi-decaying (0^+) ground states ($T_{1/2} \approx 30$ ms). There was no evidence for βp decays from the ground states of ^{90}Rh , ^{94}Ag , and ^{98}In . For the case of ^{98}In , the $b_{\beta p}$ of the ground states and the isomer differed vastly from the literature values. βp emission from ^{101}In was investigated by searching for nonzero βp contributions at late decay correlation times after ^{101}Sn implantations, and an upper limit of 1.7% was assigned to the $b_{\beta p}$ of ^{101}In .

Unlike the $T_{1/2}$ results, the $b_{\beta p}$ measured in this work deviated substantially from the literature values for several states of $^{91,92}\text{Rh}$, ^{96}Ag , $^{96,97}\text{Cd}$, and ^{98}In . A slightly higher $b_{\beta p}$ was measured for ^{101}Sn as well, differing by $\approx 3\sigma$. The most significant differences were found for the ground state and the isomer of ^{98}In , where $b_{\beta p}(^{98m}\text{In}) = 44(2)\%$ measured in this work is more than twice the previous value. This result sets a new record for the largest $b_{\beta p}$ for a given state in the vicinity of ^{100}Sn . All or a significant fraction of the previously measured $b_{\beta p}(^{98}\text{In}) = 5.5^{+0.3}_{-0.2}\%$ may have belonged to the (9^+) isomer

TABLE I. β and βp decay properties ($T_{1/2}$ and $b_{\beta p}$) of the nuclei studied in this work. The half-lives determined from β and βp decay analyses are independent measurements, and are listed separately. The literature $T_{1/2}$ and $b_{\beta p}$ are taken from NUBASE2016 [34], unless otherwise cited.

Nucleus/isomer	J^π	$T_{1/2}$ (s)				$b_{\beta p}$ (%)	
		β	βp	Combined	Literature	This work	Literature
^{87}Tc	(9/2 ⁺)	2.0(3)			2.2(2)	<0.7	
^{88}Tc	(6 ⁺)	5.8(4) ^a			6.4(8)	<0.3 ^a	
^{88m}Tc	(2 ⁺)				5.8(2)		
^{88}Ru	0 ⁺	1.9(5)			1.2 ^{+0.3} _{-0.2} [53]	<3.6	
^{89}Ru	(9/2 ⁺)	1.31(3)	1.53(11)	1.32(3)	1.5(2)	3.1(2)	3.0 ^{+1.9} _{-1.7} [10]
^{91}Ru	(9/2 ⁺)	7.6(2) ^a			8.0(4)	<0.2 ^a	
^{91m}Ru	(1/2 ⁻)				7.6(8)		
^{90}Rh	(0 ⁺)	0.029(3)			0.012 ^{+0.009} _{-0.004} [53]	<0.7	
^{90m}Rh	(7 ⁺)	0.55(3)	0.58(4)	0.56(2)	1.0 ^{+0.3} _{-0.2} [53]	9.6(10)	
^{91}Rh	(7/2 ⁺)	1.60(2) ^a	1.12(33) ^a	1.60(2) ^a	1.60(15)	0.18(4) ^a	1.3(5)
^{91m}Rh	(1/2 ⁻)				1.46(11)		
^{92}Rh	(6 ⁺)	5.60(9)	5.67(26)	5.61(8)	4.66(25)	2.2(1)	1.9(1)
^{92m}Rh	(2 ⁺)	3.18(22)	2.6 ^{+1.4} _{-0.7}	3.18(22)	0.53(37)	1.7(3)	
^{92}Pd	0 ⁺	1.06(3)	0.91(29)	1.06(3)	1.0 ^{+0.3} _{-0.2} [53]	1.6(2)	
^{93}Pd	(9/2 ⁺)	1.18(2)	1.16(2)	1.17(2)	1.15(5)	7.4(2)	7.5(5)
^{94}Pd	0 ⁺	9.1(4)			9.0(5)	<0.13	0
^{95}Pd	(9/2 ⁺)	7.4(5)			7.5(5)	0.23(5)	
^{95m}Pd	(21/2 ⁺)	13.2(4)			13.3(3)	0.71(7)	0.93(15)
^{94}Ag	(0 ⁺)	0.027(2)			0.029(6) [50], 0.026 ^{+0.026} _{-0.009} [54]	<0.2	
^{94m}Ag	(7 ⁺)	0.48(2)	0.47(2)	0.47(1)	0.55(6)	17.0(6)	≈20
^{95}Ag	(9/2 ⁺)	1.80(7)			1.76(9)	2.1(3)	2.5(3)
^{96}Ag	(8 ⁺)	4.46(4)			4.44(4)	4.4(5)	6.9(7)
^{96m}Ag	(2 ⁺)				6.9(5)	14.7(24)	15.1(26)
^{96}Cd	0 ⁺	1.02(6)			0.88(9), 0.97(9) [55]	1.7(4)	5.5(40), 1.5(5) [55]
^{96m}Cd	16 ⁺	0.54(4)	0.52(7)	0.53(3)	0.29 ^{+0.11} _{-0.10} [5], 0.45 ^{+0.05} _{-0.04} [55]	19.5(29)	11(3) [55]
^{97}Cd	(9/2 ⁺)	1.22(7)	1.08(16)	1.20(7)	1.10(8)	7.4(2)	11.8(20)
^{97m}Cd	(25/2 ⁺)	3.88(8)	3.83(8)	3.86(6)	3.8(2)	25.1(5)	25(4)
^{97n}Cd	(1/2 ⁻)	0.73(7)					
^{98}Cd	0 ⁺	9.3(1)			9.2(3)	<0.029	<0.025
^{99}Cd	(5/2 ⁺)	17(1)			16(3)	0.21(2)	0.17 ^{+0.11} _{-0.05} [56]
^{98}In	(0 ⁺)	0.030(1)			0.037(5)	<0.13	5.5 ^{+0.3} _{-0.2} [10]
^{98m}In	(9 ⁺)	0.99(7)	0.88(2)	0.89(2)	1.01(13)	44(2)	19(2)
^{99}In	(9/2 ⁺)	3.11(6)			3.1(2)	0.29(3)	0.9(4)
^{100}In	(6 ⁺)	5.60(6)	5.70(16)	5.62(6)	5.83(17)	1.66(3)	1.64(24)
^{101}In	(9/2 ⁺)				15.1(11)	<1.7	
^{101}Sn	(5/2, 7/2 ⁺)	2.18(9)	2.24(6)	2.22(5)	1.97(16)	23.6(8)	21.0(7)

^aCombined result for the ground state and the isomer.

instead, where the authors of Ref. [10] themselves admitted the rather large $b_{\beta p}$ of the superallowed Fermi-decaying (0⁺) state as surprising. This new $b_{\beta p}$ value is supported by the efficiency-corrected intensities of well-known and new γ rays in ^{97}Ag , as reported in Sec. III P. One of the conditions for a high $b_{\beta p}$ is a significant Q_{ECp} value, which represents the

energy window available for β -delayed proton emission. A maximum Q_{ECp} at 9.64(32) MeV [58] was inferred for ^{98}In out of the nuclei studied in this work, whose βp daughter is a $N = 50$ magic nucleus ^{97}Ag . In the context of the rp process, the reaction flow into ^{98}In is 1–10% for x-ray bursts and more than 10% in the steady state burning, relative to the

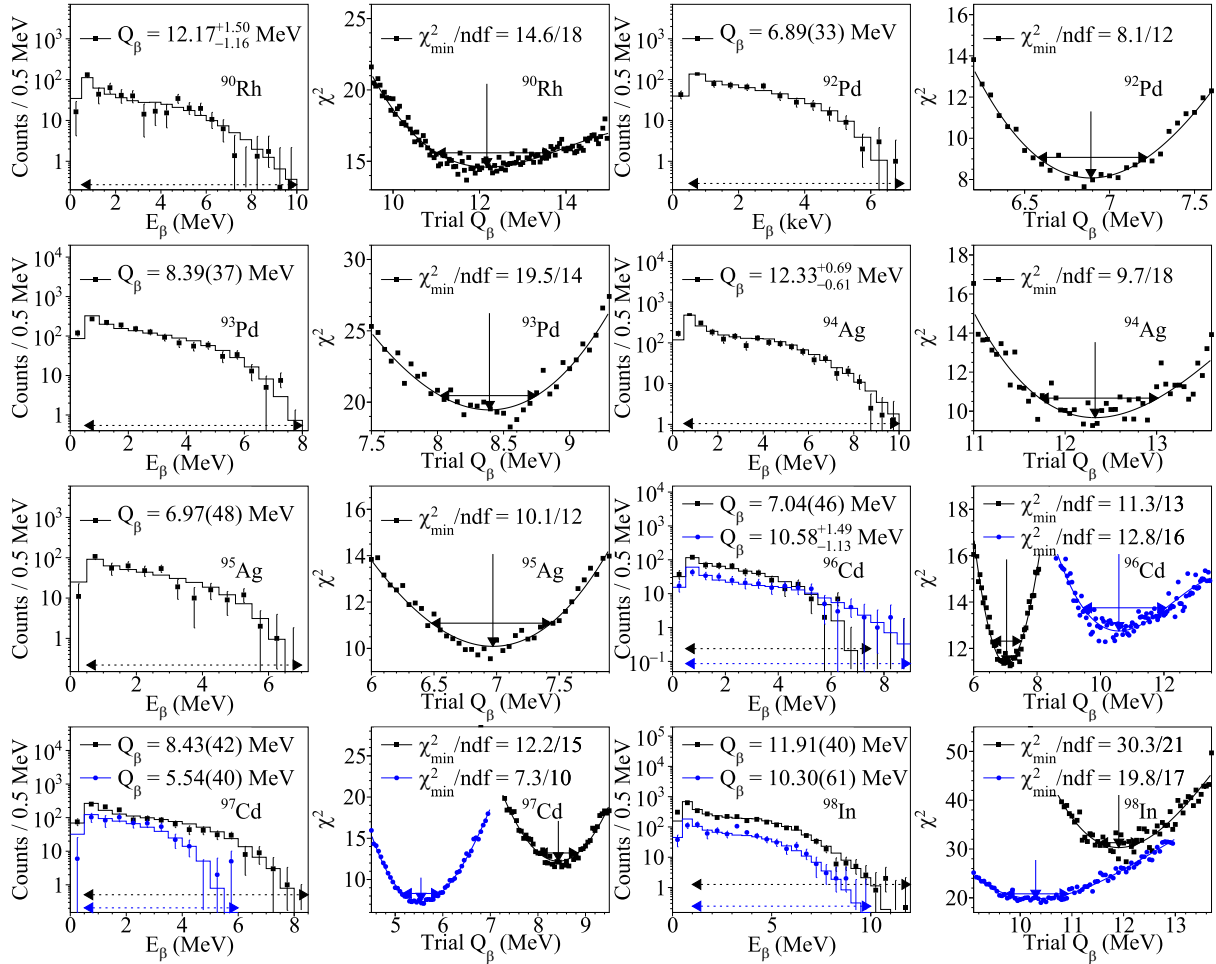


FIG. 6. Experimental γ -ray gated positron energy distributions (first and third columns) from β decays and matched Geant4-simulated energy histograms deduced from χ^2 minimization (second and fourth columns). The arrows with dotted lines indicate the χ^2 evaluation range. The vertical arrows point to the trial Q_β with the minimum χ^2 , and the horizontal arrows with solid lines represent the Q_β range where the endpoints correspond to $\chi^2 = \chi^2_{\min} + 1$ for determining 1σ uncertainties. For $^{96,97}\text{Cd}$ and ^{98}In , the Q_β of the isomeric states were also determined (round markers in blue). See Secs. II D and III C for details on the Q_β measurement methods.

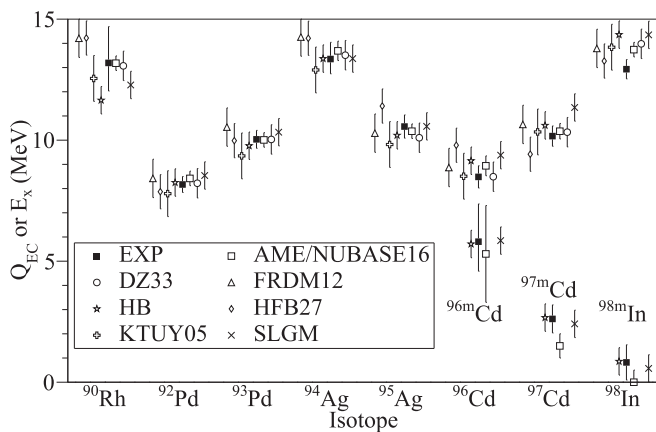


FIG. 7. Experimental Q_{EC} of the eight nuclei presented in Table II compared with different mass models [59–62], SM calculations (labeled as HB [15] and SLGM [12]) and extrapolations in AME2016 [58]. The E_x of the three isomers are also compared. See Sec. III C for descriptions of theoretical uncertainties.

reaction flow through the 3α reaction [9]. With a high $b_{\beta p}$ value for the isomer, proton capture of ^{97}Cd into ^{98m}In would result in a more abundant reaction flow to the βp daughter ^{97}Ag and eventually $A = 97$ isobars.

All of the nuclei with significant differences in $b_{\beta p}$ contain βp -decaying isomeric states, where large systematic uncertainties in β -decay and βp -decay amplitudes arise during the $T_{1/2}$ analyses which involve many more fit parameters than those without the isomeric states. Future experiments are needed to address these discrepancies.

E. Proton energy measurements in βp decays

The maximum pixel energies of identified βp decay events are shown in Fig. 8. Due to the absence of high-energy calibration of the DSSSD strips with α -decay radioactive sources, some deviations in the βp energy spectra from previous works were expected. In view of the shift of the previously reported ~ 4.5 MeV peak from the ^{97}Cd ground-state βp decay (see Fig. 10 in Ref. [10]) to ~ 5.1 MeV in this work, the inaccuracy

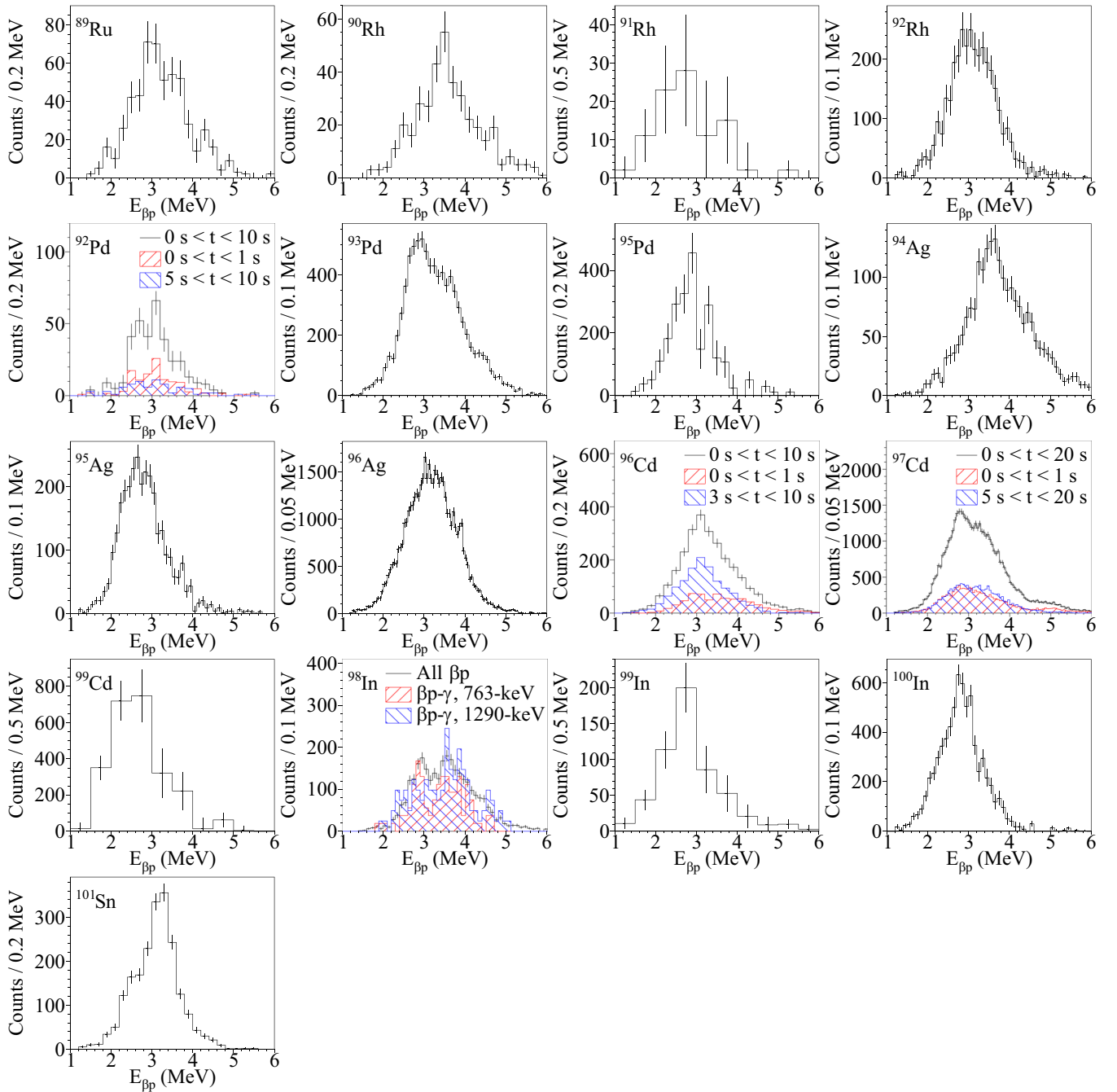


FIG. 8. WAS3ABi energy spectra of βp emitters in the ^{100}Sn region. Only the energies of the correlated pixels with the maximum ΔE are plotted. For certain nuclei, βp energy spectra with different time gates are drawn to compare the contributions from isomeric states and/or β -decay daughter nuclei. For ^{98}In , efficiency-corrected βp energy distributions with two different γ -ray gates are plotted in order to investigate the double peak structure. See Sec. III E for details.

of the proton energies is estimated to be $\sim 15\%$. The first βp energy spectra from ^{89}Ru , $^{90,91}\text{Rh}$, and ^{92}Pd decays are presented in this article, and a previously unseen double-peak structure was observed from the βp decay of ^{98m}In . By gating on the 763-keV and the 1290-keV γ rays found in the βp daughter nucleus ^{97}Ag and examining the βp energy distributions, the lower-energy peak was attributed to βp branches to the 2053-keV ($17/2^+$) state or higher lying states in ^{97}Ag .

F. β - γ spectroscopy of ^{88}Ru

One γ -ray transition following the β decay of ^{88}Ru was observed at 146.0(5) keV, as shown in Fig. 9. It was detected promptly, and the β -decay $T_{1/2}$ associated with this γ ray was 1.0(5) s—consistent with the overall half-life of 1.9(5) s.

The prompt time profile of the 146-keV γ ray suggests an EM transition with a dominant $M1$ component. The total IC coefficients calculated with BrIcc [67] for the 146-keV γ

TABLE II. β -decay daughter state energies and γ -ray gates used to determine Q_{EC} and E_x (isomers) of the 11 states presented in Fig. 6 (also see Fig. 7).

Nucleus	J^π	E_x (daughter) (MeV)	E_γ gate(s) (keV)	Q_{EC} or E_x (MeV)
^{90}Rh	(0 ⁺)	0		13.19 ^{+1.50} _{-1.16}
^{92}Pd	0 ⁺	0.257 + x	257	8.17(33) + x^a
^{93}Pd	(7/2 ⁺)	0.622	382, 622	10.03(37)
^{94}Ag	(0 ⁺)	0		13.35 ^{+0.69} _{-0.61}
^{95}Ag	(9/2 ⁺)	2.571	1220	10.56(48)
^{96}Cd	0 ⁺	0.421 + x	421	8.48(46) + x^b
^{96m}Cd	16 ⁺	2.687	257, 470, 630, 667, 1249, 1506	5.81 ^{+1.56} _{-1.22}
^{97}Cd	(9/2 ⁺)	0.716	716	10.17(42)
^{97m}Cd	(25/2 ⁺)	6.221	1306	2.62(58)
^{98}In	(0 ⁺)	0		12.93(40)
^{98m}In	(9 ⁺)	2.428	147, 198, 688, 1395	0.82(73)

^a0.05(10) MeV in Ref. [34].

^b0.00(5) MeV in Ref. [34].

ray were 0.0983(17) and 0.320(6) for $M1$ and $E2$ transitions, respectively. The IC-corrected intensity of this γ ray normalized to the number of ^{88}Ru β decays, assuming a pure $M1$ transition, was 103(76)%. SM calculations of the low-energy states in ^{88}Tc predict a 1⁺ state at 190 keV above the 2⁺ state (see Fig. 13). Based on the energy, γ -ray multipolarity, and the GT spin selection rules, a reasonable assignment of the newly observed γ ray is the (1⁺) \rightarrow (2⁺) transition in ^{88}Tc , where the (1⁺) state was populated by the ground state β decay of

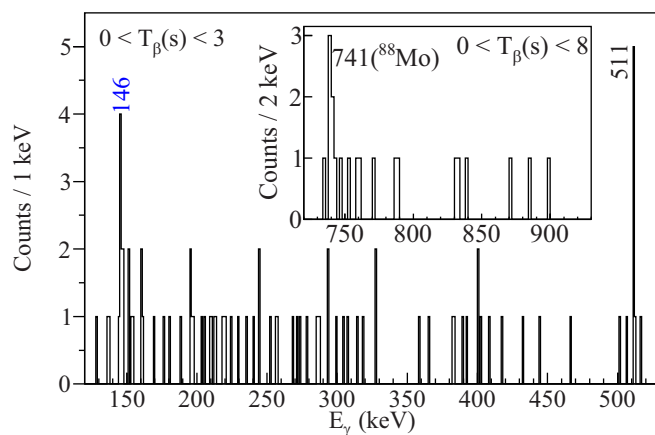


FIG. 9. β -delayed γ ray spectrum of ^{88}Ru . Note the β -decay correlation time windows for both the main plot and the inset. The 146.0(5)-keV line was assigned as the (1⁺) \rightarrow (2⁺) transition in ^{88}Tc . The inset shows the 741-keV γ ray which belongs to ^{88}Mo , the β -decay granddaughter.

TABLE III. Energies, intensities, and γ -gated half-lives of the identified γ rays from the β decay of ^{88}Tc and ^{88m}Tc . The intensities were not corrected for IC. The relative intensities, normalized to the 741-keV γ ray, are compared with Ref. [69]. See the text for details.

Energy (keV)	I_γ (%)	I_γ^{rel} (%)	$I_{\text{lit}}^{\text{rel}}$ (%)	$T_{1/2}$ (s)
444.7(5)	4.4(41)	4.3(40)	6.3(27)	7.7(31)
740.5(1)	103.4(57)	100	100	6.3(5)
914.4(1)	75.0(50)	72.5(63)	44.2(58)	6.8(7)
972.2(2)	23.9(34)	23.1(35)	18.6(36)	4.7(8)
1308.1(6)	16.6(31)	16.1(31)		6.3(13)
1507.7(6)	12.3(34)	11.9(34)		7.0(28)

^{88}Ru . The empirical $\log ft$ value of the β -decay branch to the yrast (1⁺) state in ^{88}Tc was derived to be 4.05(16) by taking $T_{1/2} = 1.9(5)$ s and assuming $b_\beta = 100\%$, $E_x(2^+) = 0$ MeV, and an extrapolated Q_{EC} value of 7.34(34) MeV [58]. The corresponding $\log ft$ value from SM calculations was 3.75, demonstrating a reasonable agreement. The properties of this new β -decay branch are similar to those of 0⁺ \rightarrow (1₁⁺) GT decays of the heavier even-even nuclei ^{92}Pd and ^{96}Cd , discussed in the later sections. Taking these findings into consideration, the spin and parity of ^{88m}Tc is proposed to be (2⁺). This assignment is further supported by the observation of the 741-keV γ ray depopulating the yrast (2⁺) state in the granddaughter nucleus ^{88}Mo , as shown in the inset of Fig. 9.

^{88m}Tc with $J^\pi = (2^+)$ is the final state proposed to be populated by the $E2$ isomeric decay from the (4⁺) state with $T_{1/2}(4^+) = 146(12)$ ns and $E_\gamma = 95$ keV [68]. SM calculations in this work predict this (4⁺) state as an isomer with $T_{1/2} = 53$ ns and $E_x = 142$ keV above the 2⁺ state, in good agreement with the experimental values. The theoretical $E2$ transition strength from the (4⁺) isomer to the (2⁺) state is approximately six times greater than that to the (6⁺) state, and taking into account $E_x^{\text{SM}}(2^+) = 0$ keV and $E_x^{\text{SM}}(6^+) = 45$ keV, 97.5% of the EM decays from the (4⁺) state is predicted to feed the (2⁺) state. The decay scheme of the (4⁺) isomer in ^{88}Tc is similar to the isomeric decay from the (4⁺) state in ^{92}Rh [22], where both of them are $T_z = (N - Z)/2 = 1$ nuclei. The theoretical ordering and the energy differences of the yrast (1⁺), (4⁺) and (2⁺) states in this nucleus are consistent with experimental observations. A measurement of the excitation energy of the (2⁺) state in ^{88}Tc will test the accuracy of the SM at $E_x \approx 50$ keV for this nucleus.

G. β - γ spectroscopy of ^{88}Tc

The β - γ spectrum of ^{88}Tc is shown in Fig. 10, and the transitions identified to belong to the daughter nucleus ^{88}Mo in this work are given in Table III. The γ -ray intensities listed in Table III are normalized to the combined number of β decays from the two states.

The yrast 2⁺ state in ^{88}Mo could be populated by either the feeding γ -ray transitions from higher states populated during the β decay of ^{88}Tc , or directly from the β decay of ^{88m}Tc whose spin-parity assignment is (2⁺) in this work.

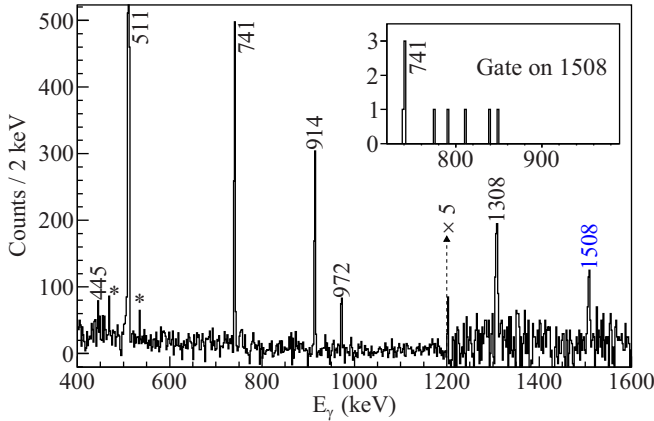


FIG. 10. β -delayed γ ray spectrum of ^{88}Tc with a correlation time window of 0–20 s. The peaks labeled in black numbers except the 511-keV annihilation peak are previously known γ -ray transitions, and those with asterisks are from long-lived and abundant species such as ^{97}Pd . The subset of the spectrum where $E_\gamma > 1200$ keV was scaled by a factor of 5 for visualization. The inset shows the coincident γ ray spectrum of the 1508-keV γ ray seen for the first time.

The combined intensity of the 741-keV γ ray depopulating this state being consistent with 100% suggests a negligible β -decay branching ratio to the ground state of ^{88}Mo from ^{88m}Tc . Furthermore, the absence of the 914-keV γ ray in the inset of Fig. 9 implies a β -decay branching ratio close to 100% for the (2_1^+) state in ^{88}Ru , identical to the β -decay spectroscopy result of ^{92m}Rh obtained in this data set (see Sec. III K).

The weak γ -ray transition at 445 keV was first reported from the β -decay spectroscopy of ^{88}Tc following fusion-evaporation reactions [69], and also seen in the $\gamma\gamma$ coincidence projection of the 741- and 914-keV transitions in this data set. The discrepancy in the relative intensities of the $4_1^+ \rightarrow 2_1^+$ 914-keV γ ray between this work and Ref. [69] can be attributed to the difference in the population ratios of the ground state and the (2^+) isomer in ^{88}Tc . In this case, the fragmentation reaction produced more ^{88}Tc in the $J^\pi \geq 5^+$ ground state than the fusion-evaporation reaction, as supported by the higher intensity of the 972-keV γ ray from a (6^+) state in ^{88}Mo and the observation of two higher-energy γ rays from states with $J^\pi \geq 4$ in this work. The known 1308-keV γ ray from the 2963-keV (6^+) state in ^{88}Mo produced in a fusion evaporation experiment [70] was observed for the first time following the β decay of ^{88}Tc . The placement of the new 1508-keV γ ray at $E_x = 2249$ keV was based on the confirmed coincidence with the 741-keV γ ray and the absence of coincidences with all other transitions. Several 2^+ and 4^+ states in ^{88}Mo with E_x between 2 and 3 MeV are predicted by SM, as shown on the right side of Fig. 13. A $\Delta J = 0$ β decay from ^{88m}Tc to a nonyrast (2^+) state in ^{88}Mo is likely, but weak transitions from higher excited states populated by the decay of the ^{88}Tc ground state to feed a (4^+) cannot be ruled out. Therefore a tentative spin assignment of $(2, 4^+)$ state in ^{88}Mo is suggested.

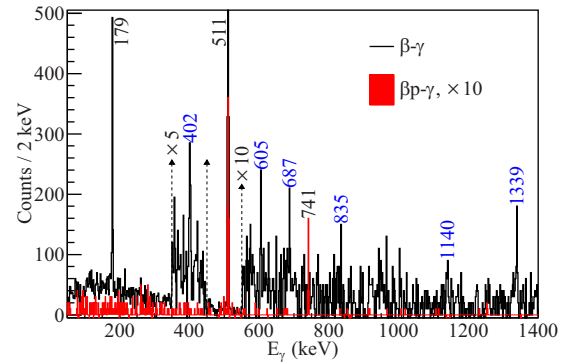


FIG. 11. γ -ray spectrum from the β decay (black line histogram) and βp decay (red filled histogram) of ^{89}Ru . The correlation time window was 0–3 s. Parts of the spectrum were zoomed with the labeled scale factors for better visualization. All labeled γ -ray peaks except those at 179 and 741 keV are new.

H. β - γ and βp - γ spectroscopy of ^{89}Ru

The first β -delayed and βp -delayed γ -ray spectroscopy results of ^{89}Ru are presented in Fig. 11. The 179-keV γ ray in the β - γ spectrum was the only transition that has been previously observed in ^{89}Tc [37], and the γ -ray peak at 741 keV observed following the βp decay of ^{89}Ru corresponds to the excitation energy of the yrast 2^+ state in ^{88}Mo discussed in the previous sections. The relative branching ratio of the βp decay from ^{89}Ru to the 2_1^+ state was measured to be 89(21)%, and no evidence for the population of higher excited states in ^{88}Mo was found. As seen from the spectrum and the intensities listed in Table IV, the six new β -delayed γ rays are quite weak. Nevertheless, $\gamma\gamma$ coincidences have been found between the 179–835- and 179–1339-keV lines.

The placement of the new transitions and the J^π assignments of new states in ^{89}Tc was limited to only a few cases, and at best inferred from SM calculations. The following three weakest γ rays without any coincidence relations were not assigned in the level scheme: 605, 687, and 1140 keV. Shown in Fig. 13 are a few calculated states in ^{89}Tc , some of which could be populated by the β decay of ^{89}Ru . A close agreement of the excitation energies between experiment and theory was found for $J^\pi \geq 7/2^+$ states, where the experimental energies of these high-spin states were measured from

TABLE IV. Energies, intensities, γ -gated half-lives, and $\gamma\gamma$ coincidence relations of the identified γ rays from the β decay of ^{89}Ru . Only the 179-keV γ ray was corrected for IC as a pure $M1$ transition.

Energy (keV)	I_γ (%)	I_γ^{rel} (%)	$T_{1/2}$ (s)	Coincidences (keV)
179.2(1)	64.7(40)	100	1.29(6)	835, 1339
401.6(4)	13.4(24)	20.7(39)	1.59(34)	
604.6(5)	4.7(16)	7.3(25)	0.96(40)	
686.6(4)	3.9(22)	6.0(34)	1.36(52)	
835.4(4)	2.9(21)	4.5(33)	0.71(35)	179
1140.0(5)	3.4(20)	5.3(31)	0.77(29)	
1339.0(5)	8.6(19)	13.3(30)	1.25(30)	179

fusion-evaporation experiments. Only one excited state with $J^\pi = 5/2^+$ was predicted at 679 keV, between the experimentally known $(7/2^+)$ and the $(13/2^+)$ states. The absence of 179–402-keV $\gamma\gamma$ coincidences, despite possessing the two highest intensities, suggests two parallel γ -decay branches. In addition, the experimental γ -ray energy of 402 keV is an intermediate value of 179 keV from the $(7/2^+)$ state and 796 keV from the $(13/2^+)$ state. Therefore a new $(5/2^+)$ state at 402 keV is proposed. The summed energy of the 179–835-keV $\gamma\gamma$ coincidence is 1014.6(4) keV, which is close to the theoretical excitation energy of the 7_2^+ state at 993 keV. The order of the $13/2_1^+ - 7/2_2^+ - 11/2_1^+$ states as predicted by SM is also consistent with this J^π assignment, with energy discrepancies less than 40 keV. Likewise, the summed energy of the 179–1339 keV $\gamma\gamma$ coincidence being 1518.2(5) keV compares well with the second-excited $5/2^+$ state predicted to lie at 1523 keV. In summary, the new energy levels and spin assignments in ^{89}Tc are shown in Fig. 13.

The ground-state spin of ^{89}Ru has been debated between $5/2^+$, $7/2^+$, and $9/2^+$ [15,71–73]. SM calculations of the level scheme of ^{89}Ru yielded excitation energies of 0, 140, and 883 keV for the yrast $7/2^+$, $9/2^+$, and $5/2^+$ states, respectively. Based on the large energy discrepancy, the $J^\pi = 5/2^+$ assignment for the ground state of ^{89}Ru is less likely. On the other hand, theoretical β -decay branching ratios are compared assuming a ground state spin of either $7/2^+$ or $9/2^+$. Direct β decays to the $(9/2^+)$ ground state of ^{89}Tc were predicted to have $b_\beta = 8\%$ and 66% from the $7/2^+$ and $9/2^+$ states, respectively. Considering the large experimental I_γ for the 179-keV, $(7/2^+) \rightarrow (9/2^+)$ transition, the $(7/2^+)$ spin assignment of ^{89}Ru is favored. The spin assignments of the new levels in ^{89}Tc are also consistent with this conclusion, where $|J_f - J_i| \leq 1$ in all cases.

I. β - γ and βp - γ spectroscopy of ^{90m}Rh

The β -delayed and βp -delayed γ -ray spectra of ^{90m}Rh are plotted in Fig. 12, and the details for each labeled transition are presented in Table V. The γ -gated decay $T_{1/2}$ results confirm that all transitions originated from the isomeric GT decay and not from the superallowed Fermi decay. The three most intense γ rays with energies of 738, 886, and 900 keV were previously known [74], and the 797.7(17)-keV line seen in the βp - γ spectrum corresponds to the known 796-keV transition from the $(13/2^+)$ state in ^{89}Tc . The two new β -delayed γ rays at 1164 and 1317 keV contained one $\gamma\gamma$ coincidence event with the 738-keV transition, plus an additional coincidence event with the 900-keV transition for the 1164-keV γ ray.

The placement of the two new γ rays was based on the coincidence relations, I_γ considerations, and the SM calculations. First, the first excited state in ^{90}Rh was predicted to be 7^+ with $E_x = 500$ keV, which would be the $\beta/\beta p$ -decaying isomer. Second, the intensity difference between the 886-keV, $6^+ \rightarrow 4^+$ γ ray and the 900-keV $4^+ \rightarrow 2^+$ γ ray in ^{90}Ru is consistent with the sum of the intensities of the two new γ rays, which suggests three parallel branches of the 886/1164/1317-keV γ rays feeding the 4^+ state. Then considering allowed GT β decays with $|J_f - J_i| \leq 1$, the

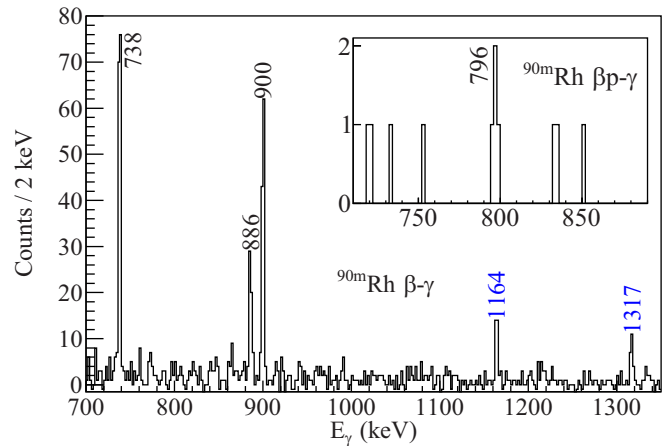


FIG. 12. γ -ray spectrum from the β decay (main plot) and βp decay (inset) of ^{90m}Rh . Two new transitions at 1164 and 1317 keV from the β - γ spectrum were found. See Sec. III I for their placements in the level scheme of ^{90}Ru .

likely spin range of the excited states in the daughter nucleus from the decay of the 7^+ isomer is $6-8^+$. As seen in Fig. 13, two 6^+ states above the yrast 6^+ state and below the yrast 8^+ state are predicted by SM. The theoretical $\log ft$ values of the isomeric decay to the three 6^+ states are 4.8, 5.3, and 4.3, in increasing order of E_x . They agree well with the experimental $\log ft$ values of $4.9^{+0.4}_{-0.3}$, $5.0^{+0.4}_{-0.3}$, and $5.1^{+0.4}_{-0.3}$, respectively, if the 1164-keV and 1316-keV γ rays are assumed to originate from the higher-lying 6^+ states. Therefore, two new (6^+) states at 2803 and 2955 keV in ^{90}Ru are proposed. When determining the experimental $\log ft$ values, the excitation energy of the ^{90m}Rh isomer was assumed to be 0.0(5) MeV according to Ref. [34].

From spin selection rules alone, the yrast 8^+ state decaying by a 512-keV γ ray to the yrast 6^+ state in ^{90}Ru could also be populated following the β decay of ^{90m}Rh . Because of the similarity of this γ -ray energy to the 511-keV annihilation γ rays and the low statistics, the β -decay branching ratio to the 8^+ state could not be measured precisely. SM predicts

TABLE V. Energies, intensities, γ -gated half-lives, and $\gamma\gamma$ coincidence relations of the identified γ rays from the β decay and βp decay of ^{90m}Rh . IC coefficients were not applied.

Energy (keV)	I_γ (%)	$T_{1/2}$ (s)	Coincidences (keV)
β -decay γ rays			
738.1(1)	100(12)	0.61(6)	886, 900, 1164, 1317
885.7(2)	41(7)	0.56(9)	738, 900
900.2(2)	85(11)	0.56(6)	738, 886, 1164
1163.9(2)	26(6)	0.61(17)	738, 900
1316.6(3)	20(6)	0.52(12)	738
βp -decay γ rays			
797.7(17)	27(15)	0.57(28)	

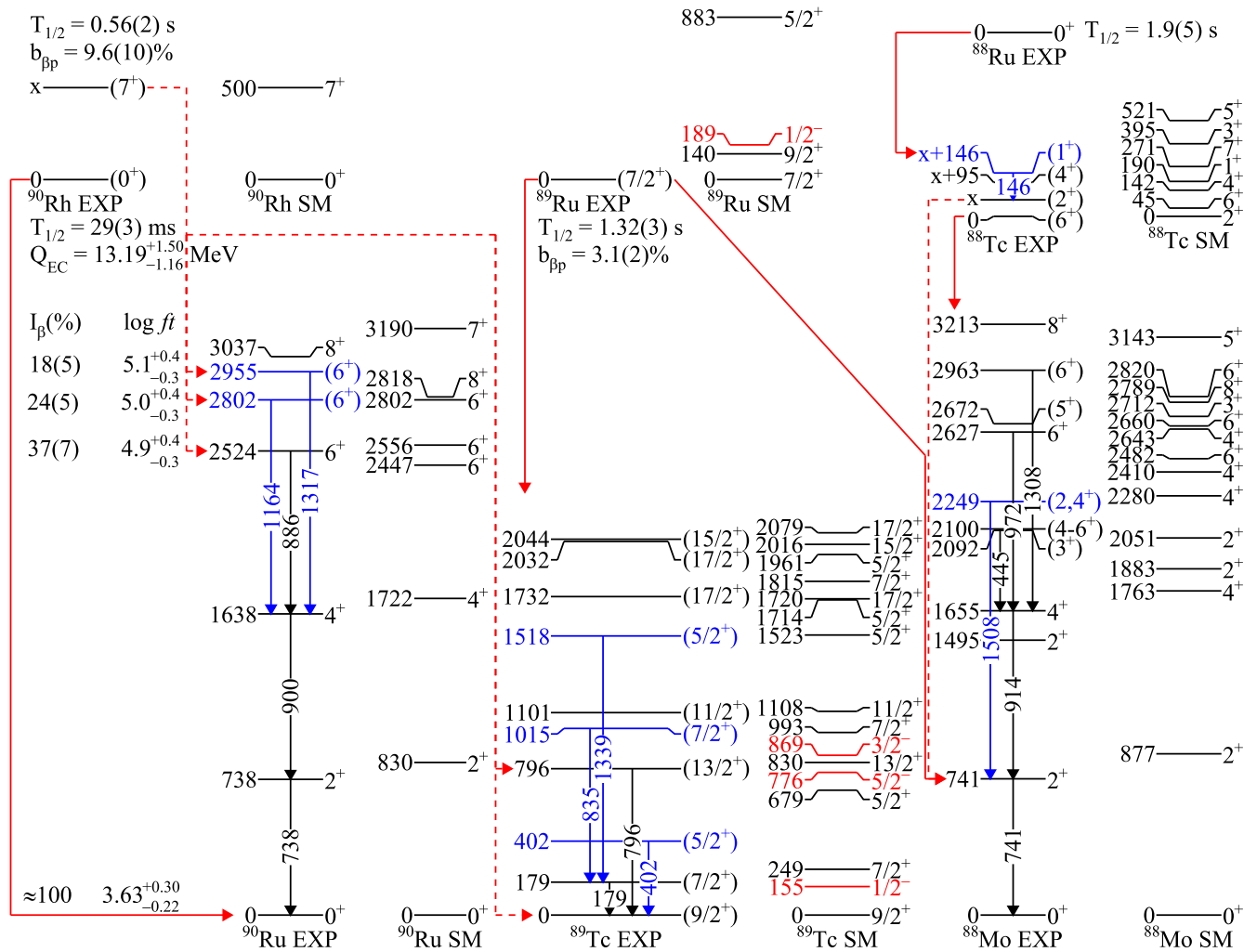


FIG. 13. Level schemes from ^{90}Rh , $^{88,89}\text{Ru}$, and ^{88}Tc decays. New γ rays and proposed states in this work are drawn in blue. States and γ rays which have been previously observed or predicted by SM are drawn in either black (for positive-parity states) and red (for negative-parity states). All excitation and γ -ray energy labels are in keV.

$\log ft = 5.3$ for this decay branch, corresponding to $b_\beta = 8\text{--}9\%$. Subtracting this hypothetical branching ratio from $b_\beta = 37(7)\%$ for the yrast 6^+ state would increase the experimental $\log ft$ by 0.1.

The population of the 796-keV ($13/2^+$) state in ^{89}Tc from the βp decay of ^{90m}Rh is also a supporting evidence for the (7^+) spin assignment of the isomer. The normalized intensity of the 796-keV γ ray is far lower than 100%, which suggests a significant $b_{\beta p}$ to the ($9/2^+$) ground state. Even though the spin difference between the initial and the final state implies an emission of positrons or protons with nonzero angular momenta, the larger Q value of the decay branch may have adequately compensated for the angular momentum barrier. The search for a βp -decay branch to the yrast ($11/2^+$) state at $E_x = 1101$ keV would require higher statistics.

J. β - γ spectroscopy of ^{91}Rh

The β - γ spectrum of ^{91}Rh is shown in Fig. 14, and the properties of the labeled peaks are given in Table VI. Just as in the case of ^{88m}Tc and ^{88}Tc , it was impossible to determine

the isomeric ratio of ^{91m}Rh because of its similar half-life compared to the ground state. The γ -ray intensities listed in Table VI were normalized to the combined number of β decays from the two states. All γ -ray intensities are consistent within 2σ compared to the literature values [75]. No $\gamma\gamma$ coincidences were observed for the six γ rays in Table VI.

SM calculations favor the ($9/2^+$) spin assignment to the ground state of ^{91}Rh , lying approximately 100 keV below the $7/2^+$ state. The b_β predictions for the ($9/2^+$) ground state of ^{91}Ru are 63% (assuming $J_i^\pi = 9/2^+$) and 14% ($J_i^\pi = 7/2^+$). The raw sum of the observed β -delayed γ -ray intensities, despite being underestimated, is 28(3)%. This result agrees much better with the large ground-state to ground-state b_β value assuming $J^\pi(^{91}\text{Rh}) = 9/2^+$. On the other hand, the yrast ($7/2^+$) state in ^{91}Ru at $E_x = 46$ keV could in principle be populated by β decays but was not observed in this work. An upper limit for this β -decay branching ratio was determined to be 5%, taking into account $\alpha = 2.87(4)$ for the 46-keV $M1$ transition. This result is also consistent with the theoretical $b_\beta = 3\%$ assuming $J^\pi(^{91}\text{Rh}) = 9/2^+$, as opposed to 45% if $J^\pi(^{91}\text{Rh}) = 7/2^+$. However, it is worth noting that the SLGM

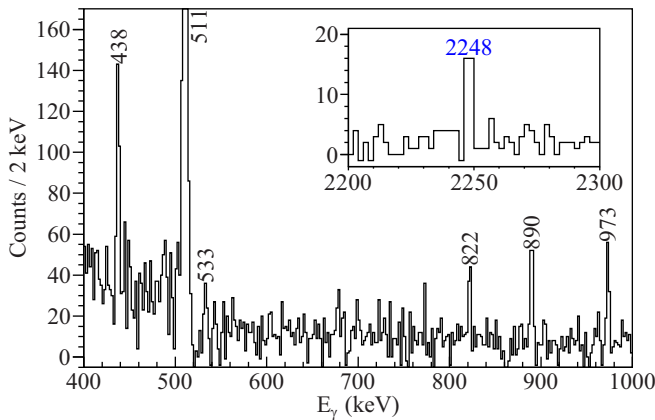


FIG. 14. β -delayed γ -ray spectrum of ^{91}Rh with a correlation time window of 0–3 s. The peaks labeled in black numbers except the 511-keV annihilation γ ray are previously known γ -ray transitions. The inset shows a new γ -ray peak at 2248 keV.

interaction fails to reproduce the order of the yrast $9/2^+$ and $7/2^+$ states in ^{91}Ru .

Both the 890-keV and 973-keV γ rays were previously assigned to depopulate the $(11/2^+)$ and $(13/2^+)$ states. Tentative assignments of the 438-, 533-, and 822-keV γ rays based on SM results are presented in this work. The newly observed γ ray at 2248 keV could not be placed in the level scheme of ^{91}Ru , since the density of states is too high in the relevant excitation energy region (see the right side of Fig. 19). The 437.7(2)- and 533.1(16)-keV transitions have significant discrepancies in energies compared to the 436.0(5)- and 538.0(5)-keV γ rays observed from the fusion-evaporation experiment [76]. Therefore they should not be equated with the 436–538 weak γ -decay cascade branch from the yrast $(13/2^+)$ state at 973 keV. The existence of the $(1/2^-)$ isomer in ^{91}Rh [77] enables β -decay branches to negative-parity excited states in ^{91}Ru . Two such states at 546 and 737 keV above the ground state are predicted, with spins $5/2^-$ and $3/2^-$, respectively. The absence of positive-parity excited states below $E_x = 1000$ keV in the SM calculations implies that the 438/533-keV γ rays are likely to originate from the aforementioned negative-parity states, populating the yrast $1/2^-$ state in ^{91}Ru . The spin assignments of the two states remains ambiguous. On the other hand, the newly ob-

TABLE VI. Energies, intensities, and γ -gated half-lives of the identified γ rays from the β decay of ^{91}Rh and ^{91m}Rh . IC coefficients were not applied on determining I_γ . The literature I_γ^{rel} and $T_{1/2}^{\text{lit}}$ values were taken from Ref. [75].

Energy (keV)	I_γ (%)	I_γ^{rel} (%)	$I_{\text{lit}}^{\text{rel}}$ (%)	$T_{1/2}^{\text{expt}}$ (s)	$T_{1/2}^{\text{lit}}$ (s)
437.7(2)	7.1(13)	100	100	1.46(15)	1.65(30)
533.1(16)	2.4(9)	34(14)	21(10)	2.05(47)	
822.1(2)	4.0(10)	56(17)	63(9)	1.50(34)	1.84(35)
890.1(3)	6.8(10)	96(22)	52(11)	2.01(32)	1.40(33)
973.2(3)	5.0(10)	70(19)	61(11)	1.47(24)	1.52(29)
2247.8(3)	2.8(8)	39(13)		2.11(46)	

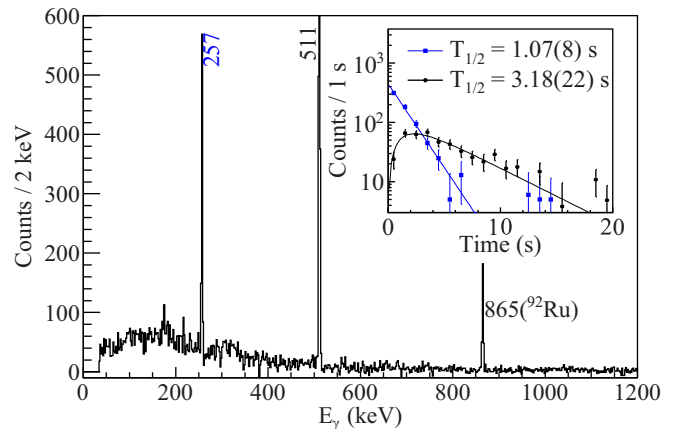


FIG. 15. β -delayed γ ray spectrum of ^{92}Pd with a correlation time window of 0–5 s. The new 257-keV γ ray was assigned as the $(1^+) \rightarrow (2^+)$ transition in ^{92}Rh . The inset shows the β -decay $T_{1/2}$ fits with the 257-keV (blue squares) and 865-keV (black dots) γ -ray gates. See Sec. III K for details.

served 822-keV γ ray is energetically similar to the excitation energies of the yrast $(3/2^-)$ and the $(5/2^+)$ states. The large uncertainty for the γ -gated β -decay $T_{1/2}$ of this transition compared to the similar half-lives of the $(9/2^+)$ ground state and the $(1/2^-)$ isomer of ^{91}Rh prevented the assignment of the parity of the parent state. Thus a new state at $E_x = 822$ keV was given a tentative J^π assignment of $(3/2^-, 5/2^+)$ as shown in Fig. 19.

K. β - γ and βp - γ spectroscopy of ^{92}Pd

The γ -ray spectrum following β decay of ^{92}Pd is shown in Fig. 15. A new γ -ray peak at 256.7(1) keV was assigned to ^{92}Rh with a β - γ half-life of 1.07(8) s, consistent with $T_{1/2}(^{92}\text{Pd}) = 1.06(3)$ s from the total β -decay half-life analysis. The intensity of the 257-keV γ ray, normalized to the total number of ^{92}Pd β decays, was 85(5)%. The IC coefficient of 0.0268(4) calculated with BrIcc was adopted for this γ ray as an $M1$ transition, for reasons stated below. No $\gamma\gamma$ coincidences were observed with this transition.

As shown in Fig. 19, SM predicts a 1^+ state with $E_x = 155$ keV above the (2^+) isomer in ^{92}Rh , with a theoretical b_β of 69% from the 0^+ ground state of ^{92}Pd to the yrast 1^+ state. Thus the 257-keV γ ray was assigned as the $(1^+) \rightarrow (2^+)$ transition in ^{92}Rh . This decay scheme was supported by the observation of the 865-keV γ ray, which was previously identified as the $(2^+) \rightarrow 0^+$ transition in ^{92}Ru [40] populated by the β decay of ^{92m}Rh . After taking into account the $b_{\beta p}$ ratio, the b_β and $\log ft$ values for the (1^+) state were determined to be 83(5)% and 4.10(10), respectively. The theoretical $\log ft$ value of 3.96 suggests a reasonable agreement. The upper limit on the b_β for the (2^+) isomer was 25%, corresponding to $\log ft > 4.7$.

By analyzing the β -decay time profile of the 865-keV γ ray, the half-life of ^{92m}Rh was measured without contributions from the ground-state decay of ^{92}Rh . As shown in the inset of Fig. 15, the resulting $T_{1/2} = 3.18(22)$ s is much longer than the literature value of 0.53(37) s [75]. In view of the

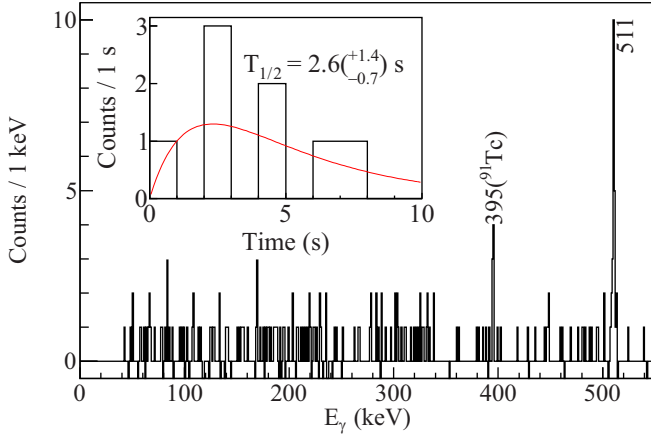


FIG. 16. βp -delayed γ ray spectrum of ^{92}Pd with a correlation time window of 0–10 s. The inset shows the βp time profile of the 395-keV γ ray belonging to ^{91}Tc and the $T_{1/2}$ fit, whose result is consistent with $T_{1/2}(^{92}\text{Rh}) = 3.18(22)$ s from β - γ analysis in Fig. 15.

$T_{1/2}(6^+) = 5.61(6)$ s deduced for the ground state of ^{92}Rh from the total β -decay time analysis, the previous half-life of 4.66(25) s [75] was likely determined by fitting a mixture of the ground state and the isomer. Another discrepancy in the intensity of the 865-keV transition was found, where $I_\gamma(865 \text{ keV}) = 102(9)\%$ normalized to the number of β decays from ^{92m}Rh supersedes the previous value of 23(10)%. Considering the small Q_β difference between the 2_1^+ and the ground state in ^{92}Ru and the angular momentum difference, the dominant β -decay branching to the 2_1^+ state is a more sensible result. Taking the updated $T_{1/2}$ and b_β , the log ft value for the ^{92m}Rh decay to the yrast (2^+) state in ^{92}Ru was deduced to be 5.15(6). Assuming $b_\beta < 15\%$ for the ground state of ^{92}Ru , the lower limit on the log ft value of the $l = 2$, (2^+) \rightarrow 0^+ β decay of ^{92m}Rh is 6.2.

The βp -delayed γ -ray spectrum of ^{92}Pd is shown in Fig. 16. Only the 395-keV deexcitation γ ray from the $7/2^+$ state in ^{91}Tc was found, which is a precursor of the βp decay of ^{92m}Rh populated by the β decay of ^{92}Pd . The corresponding β - βp half-life was $2.6_{-0.7}^{+1.4}$ s, which is consistent with the revised $T_{1/2}$ of ^{92m}Rh . The intensity of the 395-keV γ ray normalized to the number of βp decays from ^{92m}Rh was 49(36)%.

L. β - γ and βp - γ spectroscopy of ^{93}Pd

The γ -ray spectrum following the β decay of ^{93}Pd is shown in Fig. 17. The three most intense γ rays at 240, 382, and 623 keV were previously identified in a β -decay spectroscopy experiment [78], while the 894-keV γ ray was only known from the βp decay of ^{94}Ag [79]. Evidence for the known 853-keV γ -ray line in this data was inconclusive, and the previously identified transition at 864 keV [78] was not found—in agreement with the ENSDF evaluation. Instead, a new γ ray at 1301 keV was found. The details of the five unambiguous γ rays are given in Table VII.

The ground state spin of ^{93}Pd has been suggested to be either ($7/2^+$) or ($9/2^+$), with more works favoring the latter

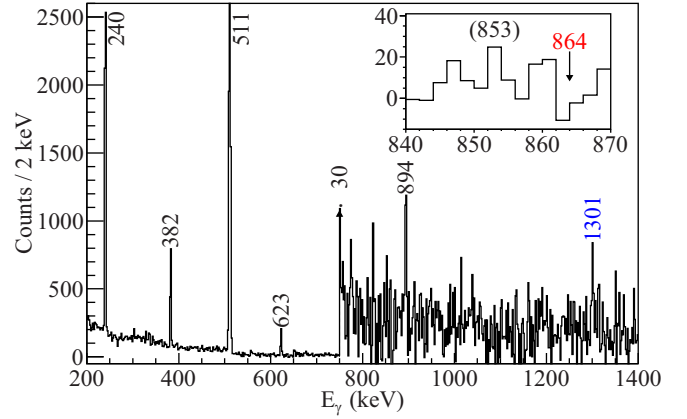


FIG. 17. β -delayed γ -ray spectrum of ^{93}Pd with a correlation time window of 0–2 s. The short correlation window was chosen to improve the signal-to-background ratio. One new γ ray was found at 1301 keV. The inset shows a possible signature of the previously identified 853-keV γ ray and the absence of the 864-keV γ ray.

[78,80,81]. From SM calculations in this study, the $7/2^+$ state was predicted to be the ground state as it lies 137 keV below the $9/2^+$ state. Theoretical b_β for the ($9/2^+$) ground state in ^{93}Rh were 5% and 74% assuming $J^\pi(^{93}\text{Pd}) = 7/2^+$ and $9/2^+$, respectively. The high I_γ value of the 240-keV γ ray from the yrast ($7/2^+$) state in ^{93}Rh is consistent with the $7/2^+$ spin assignment to the ground state of ^{93}Pd , where the experimental b_β for the yrast ($7/2^+$) and ($5/2^+$) states in ^{93}Rh presented in Fig. 19 agree quite well with SM predictions (49% and 38%, respectively). The low b_β value for the 894-keV ($11/2^+$) state compared to the 622-keV ($5/2^+$) state could also be explained by the β -decay angular momentum selection rules if $J_i^\pi = 7/2^+$.

The newly observed 1301-keV γ ray matches well the theoretical excitation energies of second-excited $7/2^+$ and $9/2^+$ states in ^{93}Rh at $E_x = 1311$ and 1384 keV, respectively. A previous spectroscopy result on the βp decay of ^{94}Ag assigned a 1451-keV state in ^{93}Rh with $J^\pi = (7/2^+)$ [79],

TABLE VII. Energies, intensities and γ -gated half-lives of the identified γ rays from the β decay and βp decay of ^{93}Pd . Only the 240-keV γ ray's intensity was corrected for IC. Relative γ -ray intensities (normalized to the 240-keV γ ray in ^{93}Rh and 865-keV γ ray in ^{92}Ru) are compared with Refs. [78,80].

Energy (keV)	I_γ (%)	I_γ^{rel} (%)	$I_{\text{lit}}^{\text{rel}}$ (%)	$T_{1/2}$ (s)
β -decay γ rays				
240.1(1)	82.2(18)	100	100	1.16(2)
382.3(1)	24.5(11)	29.8(15)	30.5(47)	1.21(5)
622.6(1)	8.2(7)	10.0(9)	11.8(27)	1.30(11)
894.1(4)	2.4(6)	2.9(7)		1.52(36)
1300.7(6)	1.9(6)	2.3(7)		1.31(33)
βp -decay γ rays				
817	<4	<5	≤ 3	
865.0(1)	82.3(49)	100	100	1.03(7)
990.4(3)	10.2(19)	12.4(24)	18.7(41)	1.01(19)

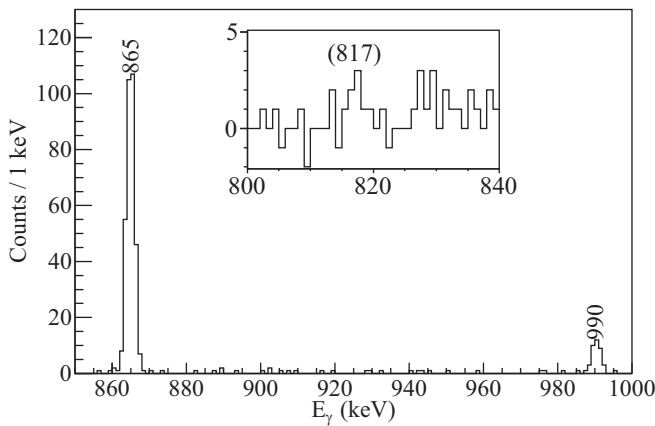


FIG. 18. βp -delayed γ ray spectrum of ^{93}Pd with a correlation time window of 0–5 s. The three labeled transitions have been reported in Ref. [80], and their intensities were used to determine experimental $b_{\beta p}$ to the excited states in ^{92}Ru .

but an alternative spin assignment of $(9/2^+)$ cannot be ruled out. With respect to the good agreement of the energies and ordering of the excited states in ^{93}Rh between experimental

data and SM, the experimental 1301-keV and 1451-keV states are assigned tentative spins $(7/2, 9/2^+)$. Above $E_x > 1500$ keV, the experimentally known states are well matched with SM calculations (see Fig. 19). The β - γ spectrum did not yield a candidate transition for an additional state predicted by SM at 971 keV with $J^\pi = 5/2^+$. If the state exists, then the intensity of the β -delayed γ ray is expected to be below 2%.

The βp -delayed γ -ray spectrum of ^{93}Pd is shown in Fig. 18. The intensities of the known γ rays in ^{92}Ru are consistent with literature values from Ref. [80], and an upper limit of 4% was assigned to the intensity of the 817-keV γ ray which is the $(6^+) \rightarrow (4^+)$ transition. The $b_{\beta p}$ are given in Fig. 19.

M. β - γ and βp - γ spectroscopy of ^{95}Ag

The γ -ray spectrum following the β decay of ^{95}Ag is shown in Fig. 20. While all of the identified γ rays have already been known, it was uncertain whether the 1571-keV γ ray belongs to the decay of ^{95}Pd or ^{95}Ag [83]. In this work, the β -decay $T_{1/2} = 1.2(4)$ s associated with the 1571-keV transition is consistent with the half-life of ^{95}Ag ; therefore it was assigned to the level scheme of ^{95}Pd . The intensities of

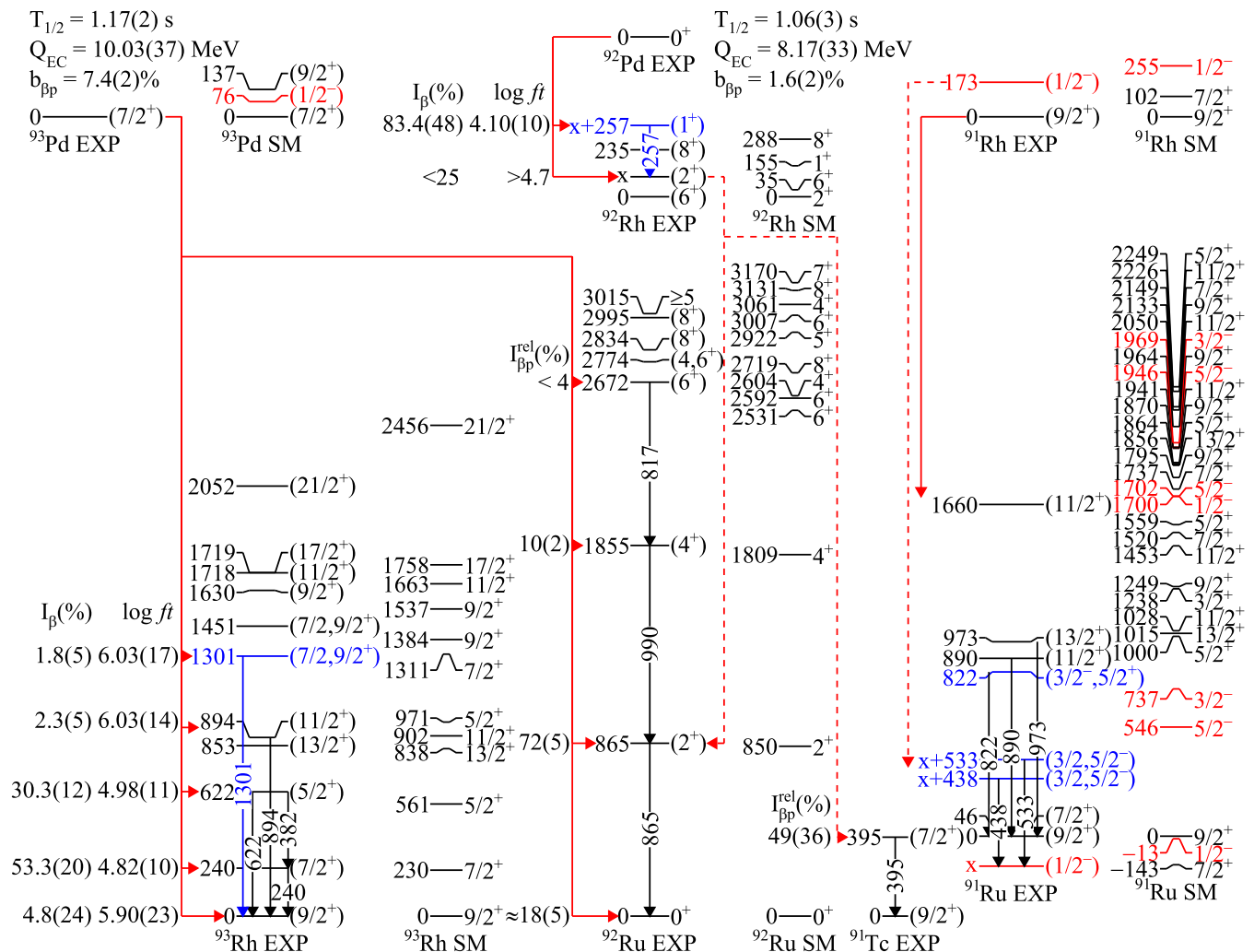


FIG. 19. Level schemes from $^{92,93}\text{Pd}$ and ^{91}Rh decays examined in this work. Additional descriptions are identical to the caption for Fig. 13.

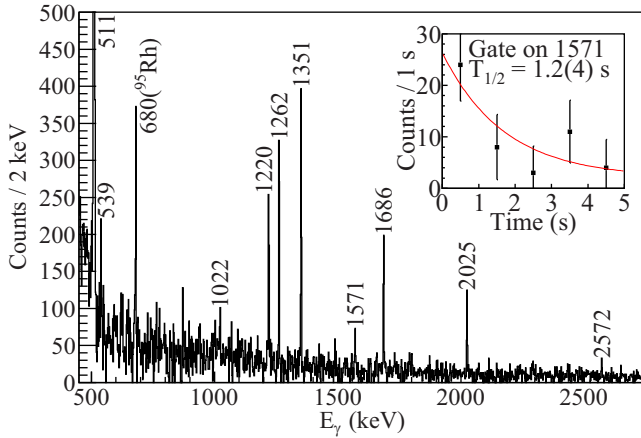


FIG. 20. γ -ray spectrum associated with the β decay of ^{95}Ag , in a correlation time window of 0.1–10 s. The nonzero start time of the correlation window was used to suppress γ -ray background from the isomeric IC decays in ^{95}Ag [82]. The inset shows the γ -gated β -decay $T_{1/2}$ of the 1571-keV γ ray, in agreement with the half-life of ^{95}Ag .

the γ rays are given in Table VIII, and the I_{γ}^{rel} are consistent with literature values.

SM calculations predict three excited states in ^{95}Pd with spins between $5/2^+$ and $9/2^+$ in the energy range of 1600–1800 keV, as shown in Fig. 24. The level of agreement in E_x between the experimental and the theoretical states below $E_x = 2700$ keV is particularly high in ^{95}Pd , where $|E_x(\text{Exp}) - E_x(\text{SM})| < 110$ keV for all states. Two states with experimental E_x of 1686 and 1801 keV have been previously assigned, making the 1571-keV γ ray a likely candidate to complete the set of excited states in this energy range. Thus a new 1571-keV state with spin and parity $(5/2, 7/2, 9/2^+)$ is proposed.

TABLE VIII. Energies, intensities, and γ -ray gated decay $T_{1/2}$ of the identified γ rays from the β decay and βp decay of ^{95}Ag . The relative γ -ray intensities are compared to the literature values [83]. IC coefficients were applied only on the βp -delayed γ rays, assumed to be $M1$ transitions.

Energy (keV)	I_{γ} (%)	I_{γ}^{rel} (%)	$I_{\text{lit}}^{\text{rel}}$ (%)	$T_{1/2}$ (s)
<i>β-decay γ rays</i>				
539.3(4)	3.2(8)	26(7)	13.9(11)	2.3(4)
1022.4(3)	2.4(7)	20(6)	14.9(13)	1.9(4)
1219.8(2)	8.7(9)	71(7)	58(3)	1.6(1)
1261.8(1)	12.3(9)	100(7)	100(5)	1.6(1)
1351.4(2)	13.3(12)	108(10)	121(7)	1.9(2)
1570.8(4)	2.9(6)	24(5)		1.2(4)
1686.4(2)	8.1(8)	66(7)	60(4)	1.7(2)
2025.0(2)	4.9(6)	40(5)	44(3)	1.8(2)
2571.5(20)	1.3(6)	11(5)	9.3(11)	1.6(4)
<i>βp-decay γ rays</i>				
196.0(3)	8.6(34)	37(15)		1.2(7)
246.6(3)	7.9(27)	34(12)		2.2(6)
315.5(2)	23.0(41)	100(18)		2.1(3)

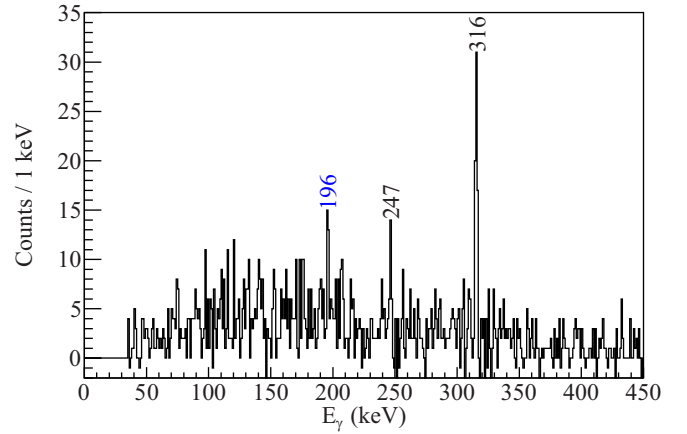


FIG. 21. γ -ray spectrum following the βp decay of ^{95}Ag , with a decay correlation window of 0–8 s. One new γ ray was found at 196 keV, and the two other labeled γ rays confirmed the previous measurement [10].

Three βp -delayed γ rays at 196, 247, and 316 keV were observed as shown in Fig. 21, where the two highest-energy γ rays were detected in a previous experiment [10]. The precise energies and the intensity of the γ rays are listed in Table VIII. The half-lives measured in coincidence with the identified γ rays were (in seconds) 1.2(7), 2.2(6), and 2.1(3), in an increasing order of γ -ray energy. All of them are consistent with the overall $T_{1/2}$ of ^{95}Ag . SM calculations propose yrast 3^+ , 5^+ , 6^+ , and 7^+ states with $E_x < 300$ keV, which are the likely parent states for the three observed γ rays. The presence of the (2^+) isomer at $E_x = 55$ keV and the (8^+) isomer with an unknown E_x resulted in arbitrary energy labels *a*, *b*, and *c* for the new excited states suggested in this work, as shown in Fig. 24. Only when higher statistics becomes available in a future experiment may possible $\gamma\gamma$ coincidence relations with the delayed 55-keV γ ray from the (2^+) state be used to deduce the excitation energies of the proposed states in ^{94}Rh . Potential βp decay branches to the $(2^+, 8^+)$ isomers and the (4^+) ground state in ^{94}Rh may also be confirmed.

N. β - γ and βp - γ spectroscopy of ^{96}Cd

The β -delayed γ rays of ^{96}Cd were separated into two sets according to the γ -ray detection time, as shown in Fig. 22. The delayed γ rays belonged to the decay cascade of the (15^+) isomer in ^{96}Ag [18], populated by the GT decay of the 16^+ isomer ^{96m}Cd [5]. Several prompt γ rays were observed for the first time at 489, 843, 3178, and 3691 keV, in addition to the previously known 421-keV transition. Taking the 68(5)% b_{β} and the measured $T_{1/2}$ and Q_{β} , the $\log ft$ value of the β -decay branch to the yrast (1^+) state was 4.21(16), generally consistent with the SM result of 4.03. No $\gamma\gamma$ coincidences were found between the prompt γ rays, due to low statistics. The excited states from which the new γ rays are emitted are most likely to be 1^+ states in ^{96}Ag , populated by the GT decay of the 0^+ ground state of ^{96}Cd . Several 1^+ states with excitation energies up to 3700 keV are predicted by SM (see Fig. 24), which may be the candidate states for the newly observed γ rays. Any higher statistics leading to more precise

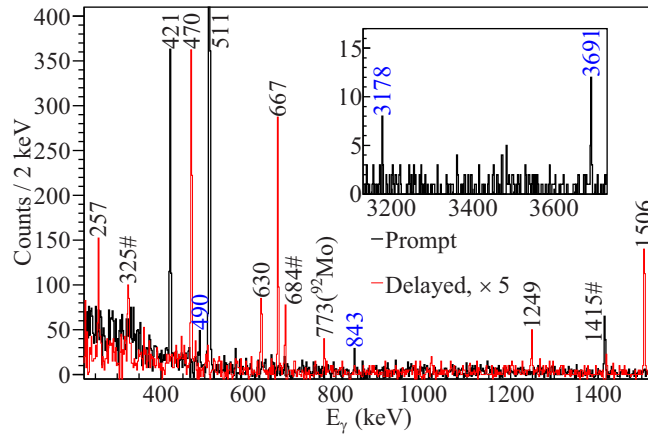


FIG. 22. γ -ray spectra associated with the β decay of ^{96}Cd , in a correlation time window of 0–5 s. The peaks with # signs indicate γ rays from the granddaughter nucleus ^{96}Pd . Black: prompt γ ray spectrum where $|T_\gamma - T_\beta| < 200$ ns. Red: delayed γ ray spectrum where $200 \text{ ns} < T_\gamma - T_\beta < 8200$ ns, scaled by a factor of 5. The peaks with blue labels are new γ rays.

$T_{1/2}$ and possible $\gamma\gamma$ coincidences will allow us in the future to firmly establish new low-spin states in ^{96}Ag . The intensities and the γ -gated β -decay half-lives of the detected γ rays are shown in Table IX.

The $\log ft$ value for the (15^+) isomer in ^{96}Ag was approximated by subtracting the experimental $b_{\beta p}$ value of ^{96m}Cd and further taking into account theoretical b_β for the GT resonance states in ^{96}Ag [55]. It was suggested that 1.4% and

TABLE IX. Energies and intensities of the identified γ rays from the β decay and βp decay of ^{96}Cd . Only the 130/257/421-keV $M1$ γ rays were corrected for IC. The intensities of the 691/821/1375-keV transitions in Ref. [55] were scaled down with $\alpha(130\text{-keV}, M1) = 0.182(3)$ for a consistent comparison.

Energy (keV)	I_γ (%)	I_γ^{rel} (%)	$I_{\text{lit}}^{\text{rel}}$ (%)	$T_{1/2}$ (s)
β -decay γ rays from the 0^+ ground state				
421.0(1)	69.0(48)	100(7)		1.03(6)
489.5(3)	4.9(30)	7.1(43)		0.85(17)
842.6(3)	5.9(23)	8.6(33)		1.51(41)
3177.9(7)	4.0(20)	5.8(29)		0.79(29)
3690.9(5)	6.8(24)	9.9(35)		1.08(26)
β -decay γ rays from the 16^+ isomer				
256.9(3)	22.4(53)	24.1(57)		0.48(10)
469.7(1)	93(9)	100(10)		0.62(7)
629.5(3)	29.5(55)	31.7(59)		0.44(11)
667.4(2)	71(9)	76(10)		0.60(9)
1248.7(3)	18.5(60)	19.9(65)		0.80(28)
1505.9(2)	73(12)	78(13)		0.63(10)
βp -decay γ rays from the 16^+ isomer				
130.1(2)	98(24)	100(24)	100(19)	0.78(13)
681	11(7)	11(7)		
691.2(2)	129(31)	132(32)	77(24)	0.54(8)
821	<12	<12	30(16)	
1375.1(4)	48(19)	49(19)	69(30)	0.47(12)

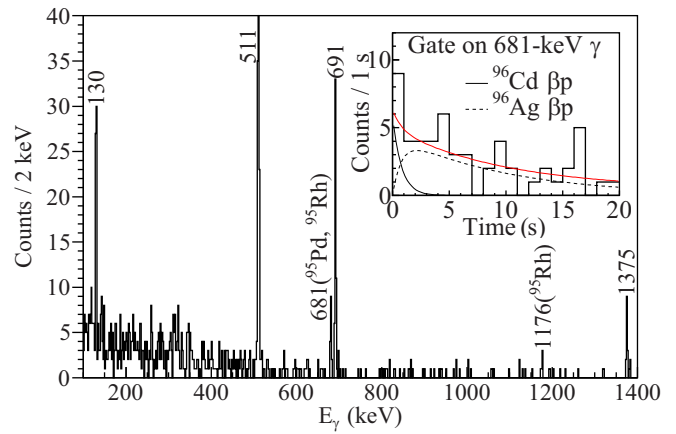


FIG. 23. γ -ray spectrum following the βp decay of ^{96}Cd , with a decay correlation window of 0–2.5 s. The inset shows the decay time profile of the unresolved γ -ray peak for the 681-keV γ ray, which was fitted with two decay components to measure the contribution from the βp decay of ^{96m}Cd .

4.3% of the β decays from the 16^+ and the 17^+ resonance states would undergo $M1/E2$ transitions to the (15^+) isomer at 2687 keV, respectively. These branching ratios were subtracted to estimate $b_\beta = 75(3)\%$ to the (15^+) isomer in ^{96}Ag , which resulted in a $\log ft$ of $4.71^{+0.40}_{-0.23}$ as shown in Fig. 24.

The βp -delayed γ -ray spectrum of ^{96}Cd is shown in Fig. 23. No γ rays from the ground state βp decay were found. The known transitions in ^{95}Pd from the βp decay of ^{96m}Cd are listed in Table IX, for intensity comparison with literature values [55]. While the 821-keV γ ray forming a parallel decay branch with the 130-691-keV cascade in ^{95}Pd was not found in these data, there was a hint of a nonzero intensity for the 680-keV γ ray from the $33/2^+$ state instead. This transition was a doublet with the 680.6(1)-keV γ ray from the βp decay of the β -decay daughter ^{96m}Ag [10]; therefore the time profile of the decay was fitted with two components in order to determine the intensity belonging to the ^{96m}Cd decay. The relative $b_{\beta p}$ of ^{96m}Cd are shown in Fig. 24.

O. β - γ and βp - γ spectroscopy of ^{97}Cd

The β -delayed γ -ray spectrum of ^{97}Cd is shown in Fig. 25. The decay correlation time window was 0–20 s. Three new transitions at 1245, 1417 (rounded down for the reason stated below), and 1673 keV were detected, and the 2013- and 2909-keV γ rays known previously from a fusion-evaporation experiment [84] were also observed in this work. Details concerning each labeled γ ray are found in Table X, and the b_β derived from the intensities of the observed γ rays are given in Fig. 29. None of the three new γ rays contained $\gamma\gamma$ coincidences with the known transitions.

The 1245-keV γ ray exhibited a γ -gated β -decay half-life of 0.73(7) s, far lower than both the literature value of 1.10(8) s and $T_{1/2} = 1.20(7)$ s measured for the $(9/2^+)$ ground state. On the other hand, the $T_{1/2}$ measured with 1417- and 1673-keV γ -ray gates were consistent with that of the ground state. The 1417.5(4)-keV β -delayed γ ray is likely

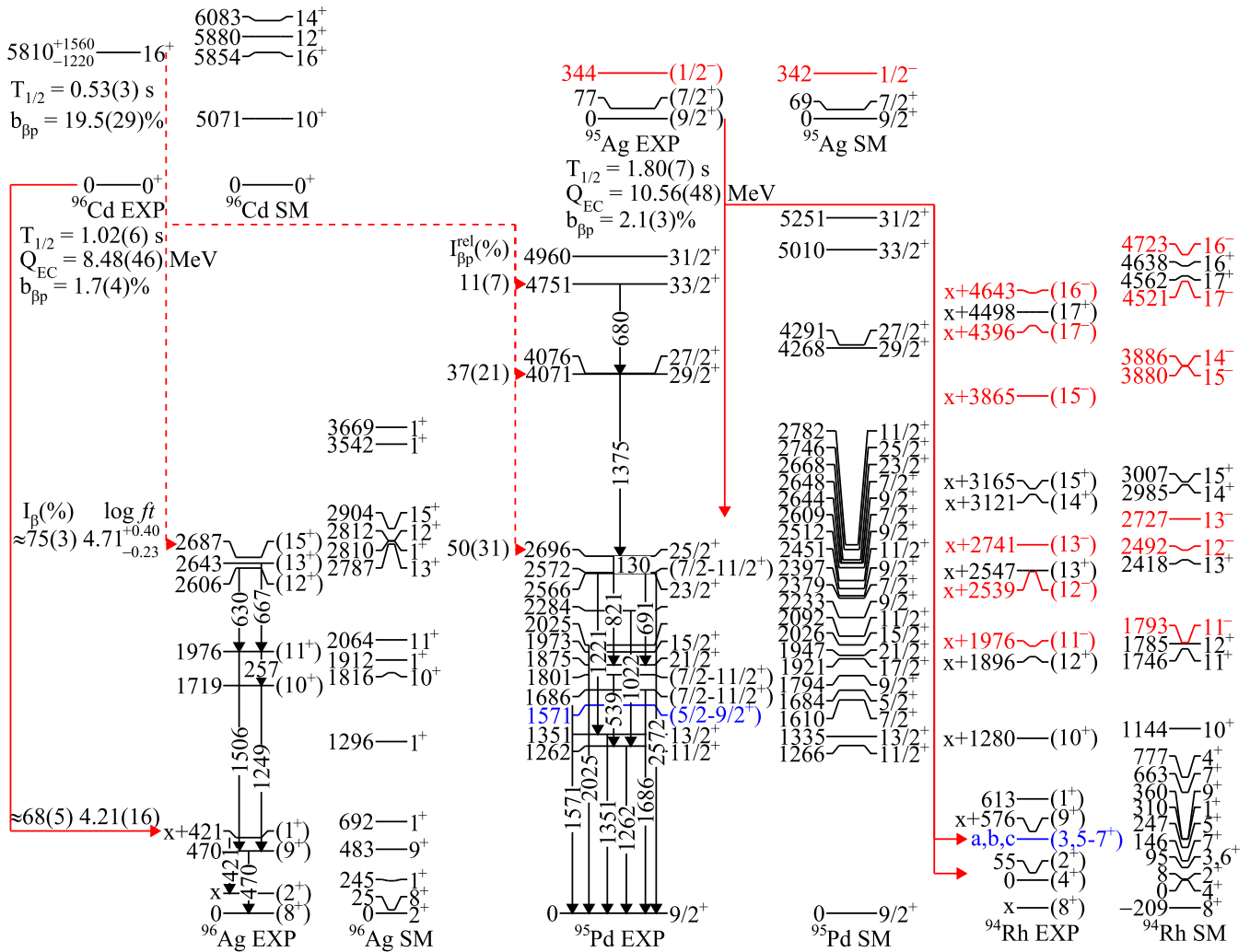


FIG. 24. Decay schemes of ^{96}Cd and ^{95}Ag decays. Three low-energy states in ^{94}Rh populated by the βp decay of ^{95}Ag with energy labels *a*, *b*, and *c* are proposed in this work. A new state in ^{95}Pd with $E_x = 1571$ keV is suggested. See Secs. III M and III N for details. New β -delayed γ rays from the ground state of ^{96}Cd were observed but could not be placed in the level scheme. SM calculations revealed several 1^+ candidate states in ^{96}Ag for these transitions.

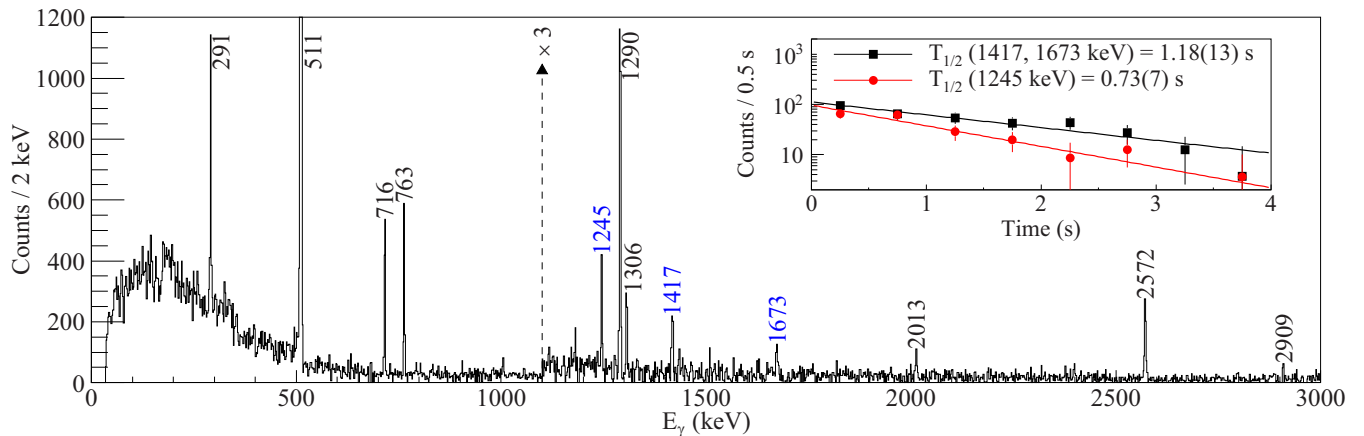


FIG. 25. β -delayed γ -ray spectrum of ^{97}Cd . The lines at 1245, 1417, and 1673 were newly observed in this work, while the previously known 2013- and 2909-keV transitions were identified for the first time from β decays. The inset shows the γ -gated β -decay half-lives of the three new transitions, indicating a short $T_{1/2}$ associated with the 1245-keV transition. See Sec. III O for details.

TABLE X. Energies and intensities of the identified γ rays from the β decay and βp decay of ^{97}Cd . Only those with $E < 400$ keV had their intensities corrected for IC. The relative γ -ray intensities are compared to the literature values [10].

Energy (keV)	I_γ (%)	I_γ^{rel} (%)	$I_{\text{lit}}^{\text{rel}}$ (%)	$T_{1/2}$ (s)
β -decay γ rays from the $(9/2^+)$ ground state				
716.1(1)	21.6(11)	100(5)		1.22(7)
1417.5(4)	4.8(9)	22(4)		1.0(2)
1673.1(5)	3.0(7)	14(3)		1.6(2)
β -decay γ rays from the $(25/2^+)$ isomer				
291.0(1)	78.4(56)	75(5)	77(10)	3.61(10)
763.0(1)	90.1(44)	86(4)	119(12)	4.00(17)
1290.0(1)	104.3(46)	100(4)	100	3.83(12)
1305.8(2)	18.6(27)	18(3)	16(4)	3.52(21)
2012.5(3)	10.9(19)	10(2)		3.49(51)
2571.6(2)	38.0(27)	36(3)	22(5)	4.26(26)
2909.4(6)	6.0(18)	6(2)		5.6(14)
β -decay γ rays from the $(1/2^-)$ isomer				
1245.1(2)	52.0(86) ^a			0.73(7)
βp -decay γ rays from the $(9/2^+)$ ground state				
683.8(1)	83.0(22) ^b	86(3)	77(5)	3.39(10)
976.7(4)	8.6(23)	9.0(24)		1.08(15)
1415.6(1)	97.0(31) ^b	100(3)	100	2.70(9)
1927.1(7)	2.1(10)	2.2(10)		1.79(55)
βp -decay γ rays from the $(25/2^+)$ isomer				
106.4(1)	108.0(43)	100(4)	100(8) ^c	3.70(14)
325.1(1)	105.4(29)	98(3)	106(6) ^c	3.72(10)
790.0(1)	32.6(16)	30(2)	27(3) ^c	4.37(27)
1253.1(1)	98.5(34)	91(3)	92(8) ^c	3.94(16)
1499.1(2)	8.6(10)	8.0(9)		3.82(52)
1740.9(6)	1.6(5)	1.5(5)		3.2(12)

^aNormalized to $N_\beta(1/2^-)$ obtained from the overall $T_{1/2}$ analysis.

^bNormalized to $N_{\beta p}(9/2^+) + N_{\beta p}(25/2^+)$, as these γ rays originate from both the ground state and the isomer βp decays.

^cNormalized from $I_{\beta p}(106 \text{ keV}) = 63(5)\%$ [10], which was presumably obtained without isolating $N_{\beta p}(25/2^+)$ from $N_{\beta p}(\text{total})$.

the same EM transition as the 1417.2(4)-keV γ ray observed from the βp decay of $^{98\text{m}}\text{In}$ (see Sec. III P), which provides supporting evidence for the said γ ray to be from the ground state decay of ^{97}Cd . The SM predicts an yrast $11/2_1^+$ and a $9/2_2^+$ state at 1525 and 1830 keV, respectively, to which the experimental γ -ray energies of 1417 and 1673 keV are assigned.

The existence of a β -decaying $(1/2^-)$ isomer in ^{97}Cd have long been hypothesized in many SM calculations [11–15], which would possess a half-life on the order of 0.1–1 s. The experimental $T_{1/2}$ associated with the 1245-keV γ ray agrees well within this range. In addition, the $(25/2^+)$ isomer in ^{97}Cd was predicted with $E_x \approx 2400$ keV by the same models, consistent with the experimental value of 2670(550) keV. The SM employed in this work yielded $b_\beta = 57\%$ for the $1/2^-$ isomer in ^{97}Cd to populate the $3/2^-$ state in ^{97}Ag , which would decay via a 1246-keV γ ray to the $1/2^-$ state. The excitation energies of the two negative-parity states are shown in Fig. 29. Both of the theoretical $1/2^-$ and $3/2^-$ states in

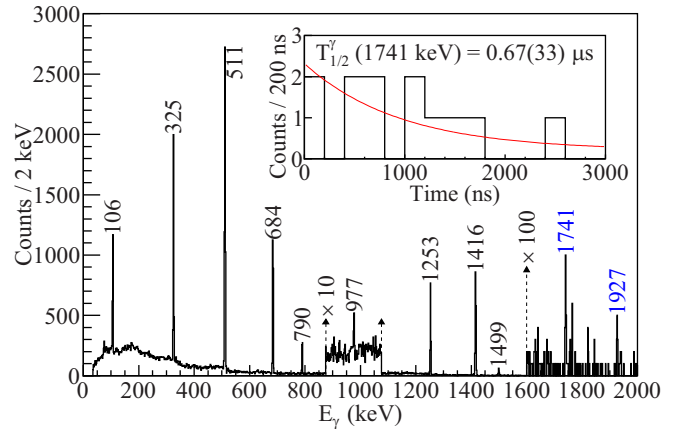


FIG. 26. βp -delayed γ -ray spectrum of ^{97}Cd . The decay correlation time window was 0–20 s, and the T_γ window was between –200 and 7500 ns. Two new γ rays were detected at 1741 and 1927 keV. The inset shows the T_γ distribution of the 1741-keV delayed γ ray and the corresponding $T_{1/2}^\gamma$.

^{97}Ag were composed of pure $\pi(p_{1/2}^- \otimes g_{9/2}^-)$ configurations. Based on the good agreement with both the $T_{1/2}$ and E_γ , the 1245-keV γ ray was assigned as the experimental deexcitation energy of the $(3/2^-)$ state to the $(1/2^-)$ state in ^{97}Ag . The half-life of 0.73(7) s assigned to the $(1/2^-)$ isomer agrees well with a theoretical prediction of 0.65 s [13] and not so for 0.08 s from Model 1 in Ref. [14]. The later model predicted an $M4$ transition from the $E_x \approx 1.3$ -MeV isomer to the $9/2^+$ ground state in ^{97}Cd . The experimental evidence for an new independent β -decay branch suggests a dominant GT decay from the isomer and thus a lower E_x , as predicted by alternative SMs as shown in Fig. 29. Unfortunately the statistics of the 1245-keV peak was too low to perform a γ -gated Q_β analysis for the $(1/2^-)$ isomer in ^{97}Cd . Likewise, signatures of βp emission from the same isomer could not be determined in these data.

The βp -delayed γ -ray spectrum of ^{97}Cd is shown in Fig. 26. Besides the known transitions up to and including the 1499-keV γ ray, two new γ rays at 1741 and 1927 keV were observed. The details of the identified γ rays are listed in Table X. The γ -gated βp half-life of the 1741-keV transition was 3.1(12) s, which is more compatible with the $T_{1/2}$ of the $(25/2^+)$ isomer. In contrast, the 1.6(5) s $T_{1/2}$ associated with the 1927-keV γ ray suggests that it was from the βp decay of the $(9/2^+)$ ground state. One $\gamma\gamma$ coincidence event was detected for each of the following pairs of transitions (in keV): 1741–1253 and 1741–684. No $\gamma\gamma$ coincidences were found for the 1927-keV γ ray due to limited statistics.

As shown in the inset of Fig. 26, the 1741-keV γ ray was delayed with $T_{1/2}^\gamma = 0.76(35)$ μs . Excluding $M1/E2$ multiplicities and assuming 100% branching for this γ ray, the experimental EM transition strengths for possible multiplicities are $8.0(37) \times 10^{-11}$ W.u. ($E1$), $5.8(27) \times 10^{-6}$ W.u. ($M2$), 0.060(28) W.u. ($E3$), and 0.20(9) W.u. ($M3$). Assuming higher multiplicities resulted in EM transition strengths that are physically unreasonable. The hypothetical $B(E3)$ was found

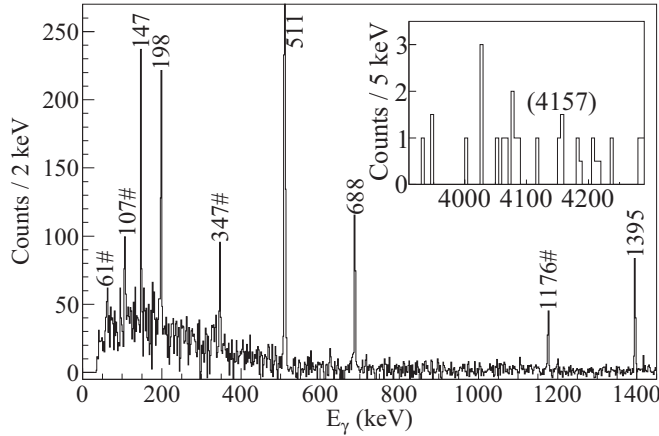


FIG. 27. E_γ spectrum following the β decay of ^{98}In , from 0 to 5 s after implantation. The γ -ray time window was $-200 < T_\gamma$ (ns) < 800 in order to observe the known γ -ray cascade from the $T_{1/2} \approx 150$ ns (8^+) isomer in ^{98}Cd . The transitions labeled with # symbols belong to ^{98}Ag . The inset shows the high-energy part of the spectrum, centered around the 4157-keV γ ray known to depopulate the (10^+) state in ^{98}Cd . See Sec. III P for details.

to be quite compatible with literature $B(E3)$ for isomeric states in this region of nuclides, such as the 267-keV γ ray in ^{95}Ag [82], the 743-keV γ ray in ^{96}Ag [18], and the 1651-keV γ ray in ^{94}Pd [21,22]. However, $M2/M3$ transitions could not be ruled out. SM calculations in the $\pi\nu(p_{1/2}, g_{9/2})$ model space could not suggest a definite parent state for the 1741-keV transition in both J^π and E_x .

A set of states in ^{96}Pd with $J^\pi = 3-6^+$ and E_x from 3200 to 3900 keV were predicted by the SM, from which the 1927-keV γ ray may be emitted feeding the yrast 2^+ state at 1415 keV. This particular range of spins offers the minimum angular momentum barrier for βp emission from the $9/2^+$ ground state of ^{97}Cd . Therefore a new state at 3342 keV with the aforementioned spin range was assigned with $b_{\beta p} = 2.1(10)\%$, along with other $b_{\beta p}$ deduced from the observed γ -ray intensities as shown in Fig. 29.

P. β - γ and βp - γ spectroscopy of ^{98}In

The γ -ray spectra following β and βp decays of ^{98}In are shown in Figs. 27 and 28, respectively. The intensities and γ -gated $T_{1/2}$ for each of the labeled transitions in each plot are listed in Table XI. In both β and βp decays, all of the observed γ rays from the parent decays are assumed to originate from the (9^+) isomer and not the (0^+) ground state which undergoes superallowed Fermi decays to the ground state of ^{98}Cd . Evidence for a 4^- isomer as predicted by SM was not found in this experiment, likely due to the high-spin ^{98}In nuclei produced from the fragmentation reaction populating the (9^+) isomer instead. The 147-198-688-1395-keV decay cascade from the (8^+) isomer in ^{98}Cd [85] was clearly observed, with I_γ being consistent with 100% for all four γ rays. Meanwhile, the search for the population of the core-excited (10^+) state

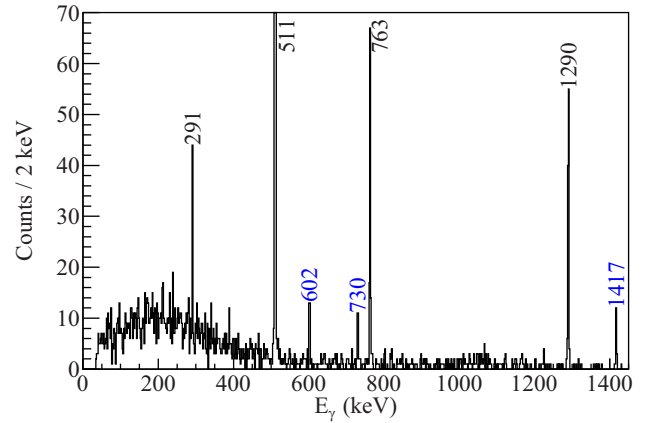


FIG. 28. E_γ spectrum following the βp decay of ^{98}In , with a correlation time window of 0–5 s. The transitions labeled in black (except the 511-keV annihilation peak) form a known γ -ray cascade of the seniority band in ^{97}Ag . Three new γ rays at 602, 730, and 1417 keV were used to establish new excited states in ^{97}Ag .

[20] did not reveal a statistically significant intensity at the corresponding γ -ray energy of 4157 keV (see the inset of Fig. 27). Therefore an upper limit of 8% was assigned to the β -decay branch to the (10^+) state. The b_β and the $\log ft$ value for the (8^+) isomer, shown in Fig. 29, were determined by assuming all non- βp branches from ^{98m}In to feed the isomer.

The most intense βp -delayed γ rays at 291, 763, and 1290 keV were previously known from the decay cascade of the yrast band in ^{97}Ag [84]. From the GT decay spin selection rule and the preference for protons to be emitted with minimum angular momentum, these γ rays also support the $J^\pi = (9^+)$ assignment to ^{98m}In . In addition, three new γ rays at 602, 730, and 1417 keV were found. To determine their placements in the level scheme of ^{97}Ag , one notes that the 127.9(5)-keV energy difference between the 730.1(4)- and the 602.2(3)-keV γ rays is consistent with the 127.1(4)-keV energy difference between the 1417.2(4)-keV and the 1290.1(2)-keV γ rays.

TABLE XI. Energies and intensities (corrected for IC) of the identified γ rays from the β decay and βp decay of ^{98m}In . γ -gated decay half-lives are also provided.

Energy (keV)	I_γ (%)	I_γ^{rel} (%)	$T_{1/2}$ (s)
<i>β-decay γ rays from the (9^+) isomer</i>			
147.2(1)	102(14)	97(13)	0.8(1)
198.4(1)	104(12)	99(11)	0.7(1)
687.8(2)	96(12)	92(11)	1.0(2)
1395.5(2)	105(11)	100(10)	0.8(1)
<i>βp-decay γ rays from the (9^+) isomer</i>			
291.1(2)	22.8(36)	26(4)	1.0(2)
602.2(3)	14.6(32)	17(4)	1.0(2)
730.1(4)	13.9(33)	16(4)	0.8(2)
762.9(2)	59.7(65)	69(7)	0.8(1)
1290.1(2)	87.0(90)	100(10)	1.0(1)
1417.2(4)	14.8(42)	17(5)	1.1(3)

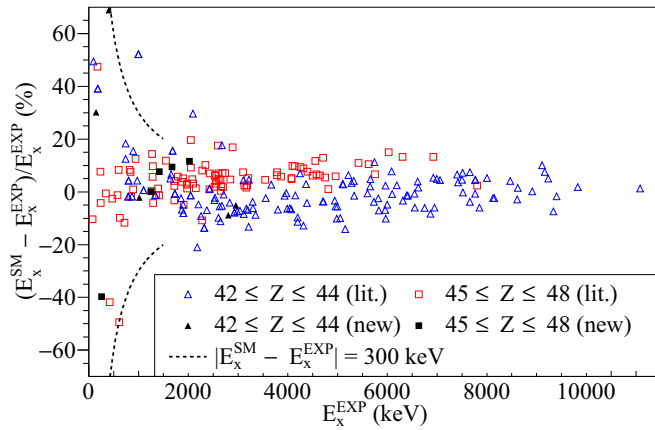


FIG. 30. Relative differences between experimental and theoretical energies of excited states in proton-rich nuclei. Only the states with unambiguous spin/parity assignments and one-to-one correspondence with SM levels are compared. The solid black markers indicate the energy discrepancies for the new states proposed in this work. The lines indicating an absolute energy difference of 300 keV for low-energy excited states are drawn also.

an extended model space and interactions for orbitals above the $N = 50$ and $Z = 50$ shell gaps. On the other hand, a slightly different trend is seen for $Z \leq 44$ nuclei. While the SM overestimates the excitation energies below 2000 keV, the excess energy decreases gradually until the experimental E_x surpasses the theoretical counterparts at higher energies. Beyond 3000 keV, the SM energies become less underestimated with a slope nearly identical to that of the $Z \geq 45$ data set. This result suggests the need to include the $\pi\nu(2p_{3/2}, 1f_{5/2})$ orbitals in the model space below the ^{76}Sr core for low-energy excited states in $Z \leq 44$ nuclei, especially for accurate predictions of low-energy negative-parity states; calculations in the $2p_{1/2}$ orbital alone for such states may not suffice. The newly proposed states in this work have excitation energy discrepancies that are well consistent with the corresponding Z -dependent trends, supporting the J^π assignments. The 402-keV ($5/2^+$) state proposed in ^{89}Tc is lower in energy compared to the predicted E_x by nearly 300 keV ($\approx 70\%$ difference), but the calculations for the same nucleus also overestimate the experimentally known $7/2^-$ state at 998 keV by $\approx 50\%$, reflecting the loss of reproducibility and predictability of SM in a limited model space for nuclei far away from the doubly magic ^{100}Sn .

IV. SUMMARY AND OUTLOOK

A decay spectroscopy experiment in the region of the doubly magic ^{100}Sn yielded many new and precise results on the half-lives, β -decay endpoint energies, and βp -decay

branching ratios. The β -decay properties of ^{92}Rh and ^{92m}Rh are revised in this work, and evidence for a β -decaying ($1/2^-$) isomer in ^{97}Cd was found. The Q_{EC} and E_x of several nuclei and isomers were consistent with various mass models, but a hint of extra stability was seen for ^{98}In . On the other hand, a large $b_{\beta p}$ was measured for ^{98m}In at over 40%, which is the (9^+) $T = 0$ pn hole spin-aligned state. The $b_{\beta p}$ discrepancies in several nuclei and their isomers exposed the large systematic uncertainties involved in multivariate analyses of the decay time distributions. More accurate and precise measurements of the decays of the daughter nuclei, as well as techniques to perform state-dependent spectroscopy, are desired.

Twenty-five new γ -ray transitions were observed from β - and βp -delayed γ -ray spectroscopy on multiple nuclei, and ten new excited states with unambiguous spins and parities are proposed based on SM calculations in the $\pi\nu(p_{1/2}, g_{9/2})$ model space. Theoretical E_x from the SLGM interaction deviated from the experimental values within 300 keV for $E_x < 2000$ keV, or 20% at higher energies. The order of the states was well reproduced in most nuclei near the proton dripline. To reduce the dependence on SM for assignment of new states and placement of other γ -ray transitions observed in this work, future decay spectroscopy experiments with higher statistics are needed.

ACKNOWLEDGMENTS

The authors would like to thank the personnel at the RIKEN Nishina Center for providing the exotic radioactive isotope beam with record intensities. This experiment was performed at RI Beam Factory operated by RIKEN Nishina Center and CNS, University of Tokyo. We acknowledge the EUROBALL Owners Committee for loaning the germanium detectors and the PreSpec Collaboration for the readout electronics of the cluster detectors of EURICA. Support for the WAS3ABi setup was provided by the Rare Isotope Science Project, funded by the Ministry of Education, Science and Technology (MEST) and National Research Foundation (NRF) of Korea, as well as KAKENHI (Grant No. 25247045) of Japan Society for the Promotion of Science (JSPS). The authors acknowledge the support of the DFG cluster of excellence ‘‘Origin and Structure of the Universe,’’ German BMBF under Contract No. 05P15PKFNA and the Spanish Ministerio de Economía y Competitividad via Project No. FPA2017-84756-C4-2-P. Part of the research was funded by the Natural Sciences and Engineering Research Council (NSERC) of Canada and also supported by FJ-NSP (French-Japanese International Associated Laboratory for Nuclear Structure Problems).

- [1] T. Faestermann, M. Górska, and H. Grawe, *Prog. Part. Nucl. Phys.* **69**, 85 (2013).
- [2] B. Cederwall *et al.*, *Nature (London)* **469**, 68 (2011).
- [3] I. Mukha *et al.*, *Nature (London)* **439**, 298 (2006).
- [4] D. Bazin, F. Montes, A. Becerril, G. Lorusso, A. Amthor, T. Baumann, H. Crawford, A. Estrade, A. Gade, T. Ginter, C. J.

- Guess, M. Hausmann, G. W. Hitt, P. Mantica, M. Matos, R. Meharchand, K. Minamisono, G. Perdikakis, J. Pereira, J. Pinter *et al.*, *Phys. Rev. Lett.* **101**, 252501 (2008).
- [5] B. S. Nara Singh *et al.*, *Phys. Rev. Lett.* **107**, 172502 (2011).
- [6] C. B. Hinde *et al.*, *Nature (London)* **486**, 341 (2012).

- [7] R. K. Wallace and S. E. Woosley, *Astrophys. J. Suppl.* **45**, 389 (1981).
- [8] H. Schatz *et al.*, *Phys. Rep.* **294**, 167 (1998).
- [9] H. Schatz, A. Aprahamian, V. Barnard, L. Bildsten, A. Cumming, M. Ouellette, T. Rauscher, F. K. Thielemann, and M. Wiescher, *Phys. Rev. Lett.* **86**, 3471 (2001).
- [10] G. Lorusso, A. Becerril, A. Amthor, T. Baumann, D. Bazin, J. S. Berryman, B. A. Brown, R. H. Cyburt, H. L. Crawford, A. Estrade, A. Gade, T. Ginter, C. J. Guess, M. Hausmann, G. W. Hitt, P. F. Mantica, M. Matos, R. Meharchand, K. Minamisono, F. Montes *et al.*, *Phys. Rev. C* **86**, 014313 (2012).
- [11] R. Gross and A. Frenkel, *Nucl. Phys. A* **267**, 85 (1976).
- [12] F. J. D. Serduke, R. D. Lawson, and D. H. Gloeckner, *Nucl. Phys. A* **256**, 45 (1976).
- [13] K. Ogawa, *Phys. Rev. C* **28**, 958 (1983).
- [14] K. Schmidt *et al.*, *Nucl. Phys. A* **624**, 185 (1997).
- [15] H. Herndl and B. A. Brown, *Nucl. Phys. A* **627**, 35 (1997).
- [16] F. Nowacki, *Nucl. Phys. A* **704**, 223 (2002).
- [17] V. I. Isakov and K. I. Erokhina, *Phys. At. Nucl.* **65**, 1431 (2002).
- [18] P. Boutachkov *et al.*, *Phys. Rev. C* **84**, 044311 (2011).
- [19] A. Blazhev, M. Gorska, H. Grawe, J. Nyberg, M. Palacz, E. Caurier, O. Dorvaux, A. Gadea, F. Nowacki, C. Andreoiu, G. deAngelis, D. Balabanski, C. Beck, B. Cederwall, D. Curien, J. Doring, J. Ekman, C. Fahlander, K. Lagergren, J. Ljungvall *et al.*, *Phys. Rev. C* **69**, 064304 (2004).
- [20] A. Blazhev *et al.*, *J. Phys.: Conf. Ser.* **205**, 012035 (2010).
- [21] T. S. Brock *et al.*, *Phys. Rev. C* **82**, 061309(R) (2010).
- [22] J. Park *et al.*, *Phys. Rev. C* **96**, 044311 (2017).
- [23] I. Ćeliković *et al.*, *Phys. Rev. Lett.* **116**, 162501 (2016).
- [24] H. Suzuki *et al.*, *Nucl. Instrum. Methods Phys. Res. B* **317**, 756 (2013).
- [25] H. Kumagai, H. Kumagai, A. Ozawa, N. Fukuda, K. Sümmerer, and I. Tanihata, *Nucl. Instrum. Methods Phys. Res. A* **470**, 562 (2001).
- [26] K. Kimura *et al.*, *Nucl. Instrum. Methods Phys. Res. A* **538**, 608 (2005).
- [27] N. Fukuda, T. Kubo, T. Ohnishi, N. Inabe, H. Takeda, D. Kameda, and H. Suzuki, *Nucl. Instrum. Methods Phys. Res. B* **317**, 323 (2013).
- [28] T. Kubo *et al.*, *Prog. Theor. Exp. Phys.* **2012**, 03C003 (2012).
- [29] C. Scheidenberger, Th. Stöhlker, W. E. Meyerhof, H. Geissel, P. H. Mokler, and B. Blank, *Nucl. Instrum. Methods Phys. Res. B* **142**, 441 (1998).
- [30] S. Nishimura, *Prog. Theor. Exp. Phys.* **2012**, 03C006 (2012).
- [31] P.-A. Söderström *et al.*, *Nucl. Instrum. Methods Phys. Res. B* **317**, 649 (2013).
- [32] T. Kurtukian-Nieto, J. Benlliure, and K.-H. Schmidt, *Nucl. Instrum. Methods Phys. Res. A* **589**, 472 (2008).
- [33] H. Bateman, *Proc. Cambridge Philos. Soc.* **15**, 423 (1910).
- [34] G. Audi, F. G. Kondev, M. Wang, W. J. Huang, and S. Naimi, *Chin. Phys. C* **41**, 030001 (2017).
- [35] T. D. Johnston and W. D. Kulp, *Nucl. Data Sheets* **129**, 1 (2015).
- [36] E. A. McCutchan and A. A. Sonzogni, *Nucl. Data Sheets* **115**, 135 (2014).
- [37] B. Singh, *Nucl. Data Sheets* **114**, 1 (2013).
- [38] E. Browne, *Nucl. Data Sheets* **82**, 379 (1997).
- [39] C. M. Baglin, *Nucl. Data Sheets* **114**, 1293 (2013).
- [40] C. M. Baglin, *Nucl. Data Sheets* **113**, 2187 (2012).
- [41] C. M. Baglin, *Nucl. Data Sheets* **112**, 1163 (2011).
- [42] D. Abriola and A. A. Sonzogni, *Nucl. Data Sheets* **107**, 2423 (2006).
- [43] S. K. Basu, G. Mukherjee, and A. A. Sonzogni, *Nucl. Data Sheets* **111**, 2555 (2010).
- [44] D. Abriola and A. A. Sonzogni, *Nucl. Data Sheets* **109**, 2501 (2008).
- [45] N. Nica, *Nucl. Data Sheets* **111**, 525 (2010).
- [46] B. Singh and Z. Hu, *Nucl. Data Sheets* **98**, 335 (2003).
- [47] E. Browne and J. K. Tuli, *Nucl. Data Sheets* **145**, 25 (2017).
- [48] B. Singh, *Nucl. Data Sheets* **109**, 297 (2008).
- [49] N. Warr, A. Blazhev, and K. Moschner, *EPJ Web Conf.* **93**, 07008 (2015).
- [50] K. Moschner *et al.*, *EPJ Web Conf.* **93**, 01024 (2015).
- [51] J. C. Hardy, L. C. Carraz, B. Jonson, and P. G. Hansen, *Phys. Lett. B* **71**, 307 (1977).
- [52] B. A. Brown and W. D. M. Rae, *Nucl. Data Sheets* **120**, 115 (2014).
- [53] P. Kienle *et al.*, *Prog. Part. Nucl. Phys.* **46**, 73 (2001).
- [54] A. Stolz *et al.*, in *Nuclear Physics in the 21st Century: International Nuclear Physics Conference INPC 2001*, AIP Conf. Proc. No. 610, edited by E. Norman, L. Schroeder, G. Wozniak, and A. M. Smith (AIP, Melville, NY, 2002), p. 728.
- [55] P. J. Davies *et al.*, *Phys. Lett. B* **767**, 474 (2017).
- [56] T. Elmroth, E. Hagberg, P. G. Hansen, J. C. Hardy, B. Jonson, H. L. Ravn, and P. Tidemand-Petersson, *Nucl. Phys. A* **304**, 493 (1978).
- [57] J. C. Hardy and I. S. Towner, *Phys. Rev. C* **91**, 025501 (2015).
- [58] M. Wang, G. Audi, F. G. Kondev, W. J. Huang, S. Naimi, and Xing Xu, *Chin. Phys. C* **41**, 030003 (2017).
- [59] P. Möller, A. J. Sierk, T. Ichikawa, and H. Sagawa, *At. Data Nucl. Data Tables* **109-110**, 1 (2016).
- [60] J. Duflo and A. P. Zuker, *Phys. Rev. C* **52**, R23 (1995).
- [61] S. Goriely, N. Chamel, and J. M. Pearson, *Phys. Rev. C* **88**, 061302(R) (2013).
- [62] H. Koura, T. Tachibana, M. Uno, and M. Yamada, *Prog. Theor. Phys.* **113**, 305 (2005).
- [63] C. Qi, *J. Phys. G: Nucl. Part. Phys.* **42**, 045104 (2015).
- [64] S. Goriely and R. Capote, *Phys. Rev. C* **89**, 054318 (2014).
- [65] J. Park *et al.*, *Phys. Rev. C* **97**, 051301(R) (2018).
- [66] K.-H. Schmidt, C.-C. Sahn, K. Pielenz, and H.-G. Clerc, *Z. Phys. A* **316**, 19 (1984).
- [67] T. Kibédi, T. W. Burrows, M. B. Trzhaskovskaya, P. M. Davidson, and C. W. Nestor Jr., *Nucl. Instrum. Methods Phys. Res. A* **589**, 202 (2008).
- [68] A. B. Garnsworthy *et al.*, *Phys. Rev. C* **80**, 064303 (2009).
- [69] A. Odahara *et al.*, *Z. Phys. A* **354**, 231 (1996).
- [70] M. Weiszflog *et al.*, *Z. Phys. A* **342**, 257 (1992).
- [71] P. Möller, J. R. Nix, and K.-L. Kratz, *At. Data Nucl. Data Tables* **66**, 131 (1997).
- [72] N. Mărginean, C. Rusu, D. Bucurescu, C. Rossi Alvarez, C. A. Ur, D. Bazzacco, S. Lunardi, P. Pavan, G. deAngelis, M. Axiotis, E. Farnea, A. Gadea, M. Ionescu-Bujor, A. Iordachescu, W. Krolas, T. Kroll, S. M. Lenzi, T. Martinez, R. Menegazzo, D. R. Napoli *et al.*, *Phys. Rev. C* **70**, 044302 (2004).
- [73] S. W. Xu, Z. K. Li, Y. X. Xie, Q. Y. Pan, W. X. Huang, X. D. Wang, Y. Yu, Y. B. Xing, N. C. Shu, Y. S. Chen, F. R. Xu, and K. Wang, *Phys. Rev. C* **71**, 054318 (2005).
- [74] D. Bucurescu, N. Mărginean, C. Rossi Alvarez, Y. Sun, C. A. Ur, L. C. Mihăilescu, G. Suliman, D. Bazzacco, S. Lunardi,

- G. deAngelis, M. Axiotis, E. Farnea, A. Gadea, M. Ionescu-Bujor, A. Iordachescu, W. Krolas, T. Kroll, S. M. Lenzi, T. Martinez, R. Menegazzo *et al.*, *Phys. Rev. C* **69**, 064319 (2004).
- [75] S. Dean *et al.*, *Eur. Phys. J. A* **21**, 243 (2004).
- [76] Y. Zheng, G. de France, E. Clément, A. Dijon, B. Cederwall, R. Wadsworth, T. Bäck, F. Ghazi Moradi, G. Jaworski, B. M. Nyakó, J. Nyberg, M. Palacz, H. Al-Azri, G. de Angelis, A. Ataç, Ö. Aktaş, S. Bhattacharyya, T. Brock, P. J. Davies *et al.*, *Phys. Rev. C* **87**, 044328 (2013).
- [77] N. Mărginean, C. Rusu, D. Bucurescu, C. Rossi Alvarez, C. A. Ur, D. Bazzacco, S. Lunardi, P. Pavan, G. de Angelis, M. Axiotis, E. Farnea, A. Gadea, M. Ionescu-Bujor, A. Iordăchescu, W. Krolas, Th. Kröll, S. M. Lenzi, T. Martinez, R. Menegazzo, D. R. Napoli, B. Quintana, P. Spolaore, Y. H. Zhang, and J. Wrzesinski, *Phys. Rev. C* **72**, 014302 (2005).
- [78] K. Schmidt *et al.*, *Eur. Phys. J. A* **8**, 303 (2000).
- [79] I. Mukha, L. Batist, E. Roeckl, H. Grawe, J. Döring, A. Blazhev, C. R. Hoffman, Z. Janas, R. Kirchner, M. La Commara, S. Dean, C. Mazzocchi, C. Plettner, S. L. Tabor, and M. Wiedeking, *Phys. Rev. C* **70**, 044311 (2004).
- [80] S.-W. Xu, Z.-K. Li, Y.-X. Xie, X.-D. Wang, B. Guo, C.-G. Leng, and Y. Yu, *Eur. Phys. J. A* **11**, 375 (2001).
- [81] C. Rusu, N. Mărginean, D. Bucurescu, C. Rossi Alvarez, C. A. Ur, D. Bazzacco, S. Lunardi, G. de Angelis, M. Axiotis, E. Farnea, A. Gadea, M. Ionescu-Bujor, A. Iordăchescu, W. Krolas, Th. Kröll, S. M. Lenzi, T. Martinez, R. Menegazzo, D. R. Napoli, P. Pavan, M. De Poli, B. Quintana, and J. Wrzesinski, *Phys. Rev. C* **69**, 024307 (2004).
- [82] J. Döring, H. Grawe, K. Schmidt, R. Borcea, S. Galanopoulos, M. Górska, S. Harissopulos, M. Hellström, Z. Janas, R. Kirchner, M. La Commara, C. Mazzocchi, E. Roeckl, and R. Schwengner, *Phys. Rev. C* **68**, 034306 (2003).
- [83] S. Harissopulos, J. Döring, M. La Commara, K. Schmidt, C. Mazzocchi, R. Borcea, S. Galanopoulos, M. Górska, H. Grawe, M. Hellström, Z. Janas, R. Kirchner, E. Roeckl, I. P. Johnstone, R. Schwengner, and L. D. Skouras, *Phys. Rev. C* **72**, 024303 (2005).
- [84] M. Lipoglavšek, M. Vencelj, C. Baktash, P. Fallon, P. A. Hausladen, A. Likar, and C.-H. Yu, *Phys. Rev. C* **72**, 061304(R) (2005).
- [85] M. Górska, M. Lipoglavšek, H. Grawe, J. Nyberg, A. Ataç, A. Axelsson, R. Bark, J. Blomqvist, J. Cederkäll, B. Cederwall, G. de Angelis, C. Fahlander, A. Johnson, S. Leoni, A. Likar, M. Matiuzzi, S. Mitarai, L.-O. Norlin, M. Palacz *et al.*, *Phys. Rev. Lett.* **79**, 2415 (1997).